Assimilation of ASCAT soil moisture products into the SIM hydrological platform

H-SAF Associated Scientist Program (AS09_01)
Final Report

23 December 2010

Draper, C., Mahfouf, J.-F., Calvet, J.-C., and Martin, E.

CNRM/GAME (Météo-France, CNRS), Toulouse, France.

METEO FRANCE
Toujours un temps d'avance

The EUMETSAT Network of Satellite Application Facilities
H SAF
Support to Operational Hydrology and Water Management

1 Introduction

The European Organisation for the Exploitation of Meteorological Satellites (EUMETSAT) Satellite Application Facility on Support to Operational Hydrology and Water Management (H-SAF) was established in late 2005, with the objectives of providing new satellite-derived products for use in operational hydrology, and performing independent validation of these products. The latter objective includes assimilating satellite-derived products into hydrological models, and assessing the impact of the new satellite-derived products on hydrological applications. Within this framework, this report presents an assessment over France of the 12.5 km Advanced SCATtermoeter (ASCAT) near-surface soil moisture product disseminated by EUMETSAT (the SM OBS1 product).

The ASCAT near-surface soil moisture data set, which provides a measure of the degree of saturation in the near-surface soil layer, is initially assessed by comparison to time series of in situ soil moisture observations from the 12 monitoring stations that make up the SMOSMANIA network in the south of France. However, the conclusions that can be drawn from this comparison are limited by the restricted spatial cover of the in situ observations, as well as the substantial representativity errors between the soil moisture quantities observed by remote and in situ sensors. Consequently an alternative approach to evaluating the ASCAT soil moisture is pursued, using output from the SAFRAN-ISBA-MODCOU (SIM) hydrological modeling suite over France. First, the ASCAT soil moisture data are compared to the near-surface soil moisture from SIM to check for consistency between the two; while any discrepancies between these two independently generated soil moisture estimates cannot be attributed to errors in either data set, a strong agreement between them suggests that both have good accuracy.

Following this, the ASCAT data are assimilated into the SIM model, to test whether this improves the hydrological forecasts from the model. Specifically, the root-zone soil moisture in the ISBA land surface model is analysed over a three and a half year period, by assimilating the ASCAT soil moisture observations with a Simplified Extended Kalman Filter. The results of the assimilation are then compared to the corresponding forecasts from the ISBA model forced with a higher quality data set. Forecasts of the soil moisture and surface water fluxes, including the river discharge generated by routing the ISBA output through the MODCOU model, are considered. If assimilating the ASCAT data can correct the ISBA/MODCOU forecasts in response to errors in the lesser quality forcing that has been used, this provides strong evidence that the ASCAT data are accurately detecting temporal changes in the near-surface soil moisture over France.

2 Data and Models

2.1 ASCAT remotely sensed soil moisture

ASCAT is a real aperture backscatter radar at 5.255 GHz (C-band), orbiting on EUMETSAT's Meteorological Operational (MetOp) satellite. MetOp is in a sun-synchronous orbit, with equator crossing times of approximately 21:30 local time for the ascending overpass and 09:30 for the descending overpass. ASCAT observes 82% of the globe each day, at 25 km resolution (resampled to a 12.5 km grid). ASCAT was launched in 2007 to replace the European Remote Sensing Satellites, ERS-1/2, which also observed C-band radar backscatter although at lower spatial resolution (50 km, resampled to 25 km). Soil moisture information can be derived from ASCAT backscatter coefficients, using the empirical change detection approach developed at the Vienna University of Technology (TU-Wien) by Wagner et al. (1999). This approach is based on the assumption that over a long data record, the highest observed reflectivity can be equated to the maximum soil moisture, while the lowest reflectivity can be equated to the minimum soil moisture, and a linear relationship can be used to interpolate the values in between (for full details refer to Wagner et al. (1999) and Naeimi et al. (2009)). The result is an observation, loosely defined as the "degree of saturation", which is scaled between 0% (the minimum soil moisture) and 100% (the maximum soil moisture), and can be converted to a volumetric soil moisture if the local soil moisture parameters are known. The ASCAT observations will be referred to throughout this report as a 'surface degree of saturation' (SDS) and reported in percentage units, to avoid confusion with volumetric (m^3m^{-3}) measures of soil moisture. Note that the SDS is localised, in that equivalent values at different locations do not necessarily indicate equivalent soil moisture, due to possible spatial differences in soil porosity.

Soil moisture information can only be retrieved from microwave observations in regions not covered by snow, a frozen surface layer, dense vegetation, and/or a significant area of standing water. Additionally, C-band microwave observations are sensitive to soil moisture in a thin surface layer, of up to 2 cm depth, hence the ASCAT observations are representative of this thin surface layer only. A deeper layer soil wetness value is often extrapolated from the observed ASCAT/ERS SDS time series using an exponentially weighted moving average filter (e.g. Wagner et al. (1999); Ceballos et al. (2005); Albergel et al. (2008)), however only the near-surface SDS is presented in this report.

The change detection method used to retrieve the SDS from backscatter observations uses a set of predefined model parameters derived from historical observations. This method was initially developed for ERS backscatter observations, and the model parameters were based on eight years (1991 - 2007) of ERS-1/2 data (Wagner et al., 1999). Since the basic measurement principles for the ERS and ASCAT instruments are the same, the initial ASCAT soil moisture products used the model parameters derived from the ERS scatterometer data set (Bartalis et al., 2007). However, the resolution and radiometric calibration of two instruments differ, resulting in small-scale artifacts associated with strong backscatter gradients in the ASCAT retrievals, as well as a strong incidence angle dependent bias associated with a swath location based instrument error (Wagner et al., 2010). In response to these issues, TU-Wien has recently updated the change-detection model parameters, based on two years (2007 - 2008) of ASCAT observations.

A handful of studies have evaluated the ASCAT soil moisture data, most of which have used the initial ASCAT data set derived using the older ERS model parameters (referred to in this report as ASCAT(ERS)). Initial qualitative evaluation showed that the ASCAT(ERS) SDS data can correctly identify large scale soil moisture climate anomalies (Bartalis et al., 2007), and it has good agreement with soil moisture derived from the TOPKAPI model over south Africa (Sinclair and Pegram, 2010). Additionally, comparison to in situ observations from 11 SMOSMANIA monitoring sites showed significant correlations over eight-months (Albergel et al., 2009) and two years (Albergel et al.,

2010b). For the updated ASCAT model parameters (referred to here as ASCAT(ASCAT)), Brocca et al. (2010b), who found that soil wetness data derived from ASCAT(ASCAT) agreed very well with in situ observations and model simulations at three locations in Italy. Additionally, Brocca et al. (2010a) obtained similarly encouraging results by also comparing the ASCAT(ASCAT) data to in situ observations from Luxembourg and Spain.

The ASCAT level 2 surface degree of saturation (SM OBS1) product, supplied directly by TU-Wien, has been used in this report. The 25 km resolution (reported on a 12.5 km grid) research product has been used, rather than the 50 km (25 km grid) operational product. Suitable quality control is vital to the successful assimilation (and assessment) remotely sensed soil moisture data, and the preparation of the ASCAT data will be described in detail in Section 3.1.

2.2 SMOSMANIA in situ soil moisture monitoring network

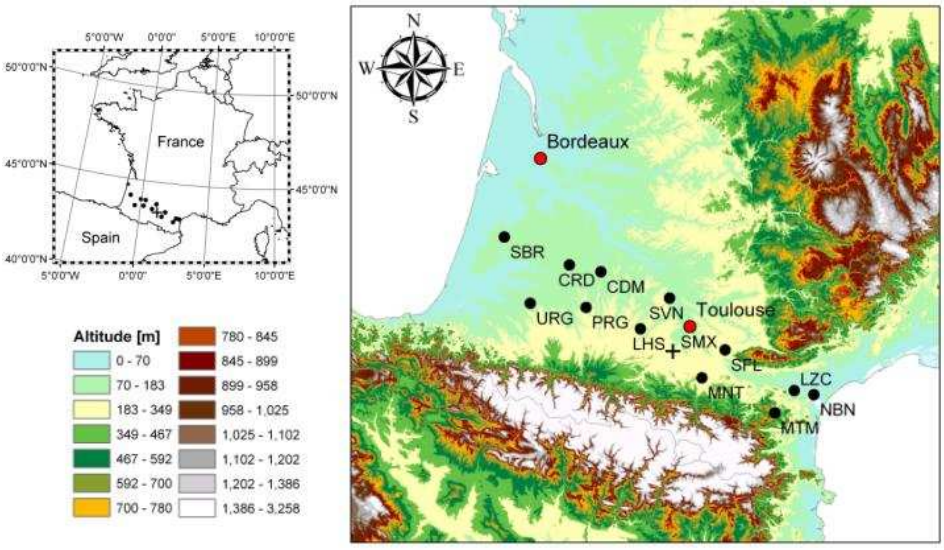

Figure 1. Location of SMOSMANIA monitoring network stations with altitude overlay. Figure taken from Albergel et al (2010).

The SMOSMANIA network (Calvet et al., 2007; Albergel et al., 2008) consists of 12 soil moisture monitoring stations in southwest France, each of which is collocated with an automatic weather station. The stations, shown in Figure 1, span a range of climates from the Mediterranean to the Atlantic coasts, and are separated by about 45 km. All of the stations are located in natural fallow. As can be seen in Figure 1, most of the stations are at low altitude and in reasonably flat terrain, with the exceptions being MTM (at 538 m), SFL (337 m), and MNT (295 m) which are at higher altitude. Each monitoring station reports soil moisture observations every 12 minutes from four theta-probes, at 5, 10, 20, and 30 cm depth. For the period of this study, the only significant period of missing data from the SMOSMANIA network is a two month period missing from LZC in mid 2007.

2.3 The SIM hydrological model

SIM (Habets et al., 2008) is a hydrometeorological model consisting of three components; a meteorological analysis (the Système d'analyse fournissant des resneignements atmospherériques à la neige; SAFRAN), a land surface model (Interactions between Surface, Biosphere, and Atmosphere: ISBA), and a hydrogeological model (MODCOU). The SAFRAN analysis system (Quintana-Seguí et al., 2008) generates analyses of the eight parameters necessary for forcing the land-surface model (10-m, wind speed, 2-m relative humidity, 2-m air temperature, cloudiness, incoming solar and atmospheric radiations, snowfall and rainfall). These analyses are then used to force the ISBA land surface scheme (Noilhan and Planton, 1989; Noilhan and Mahfouf, 1996), which models the exchanges of heat and moisture between the low-level atmosphere, vegetation, and soil. ISBA is the land surface scheme used in Météo-France's numerical weather prediction and climate models. The version used in SIM is the three layer force-restore ISBA model (Boone et al., 1999), fitted with sub-grid runoff, drainage, and explicit multilayer snow models. Finally, MODCOU computes the spatial and temporal evolution of the piezometric level of multilayer aquifers, as well as the exchanges between aquifers and rivers, before routing the surface water through the river network. River flows are calculated every 3 hours, while the evolution of the aquifers is computed daily. Evaluation studies have demonstrated that SIM can accurately reproduce the spatial and temporal variability of observed water fluxes (Habets et al., 2008), as well as the temporal dynamics of near-surface soil moisture (Rüdiger et al., 2009, Albergel et al, 2010b).

Operationally, the SIM modeling suite is run once daily to calculate the surface water and energy budgets over France, as well as the hourly land surface states (including soil moisture), three hourly stream flow forecasts for over 900 rivers, and daily aquifer levels for selected aquifers. SIM runs on a stretched (irregular) grid, with approximately 0.07º resolution. There are two operational SAFRAN analyses: the near-real time chain and the delayed cut-off climatological chain. For the near real-time chain, the SAFRAN analysis ingests all relevant observations available before the observation cut-off time, while the climatological chain is run on a delayed schedule, allowing SAFRAN to ingest additional observations from 3000 climatological observing network stations. In this report the near-real time chain has been used, for both the comparison to the SMOSMANIA and ASCAT observations in Sections 4 and 5, and for the assimilation experiments in Section 6. The delayed cut-off climatological chain has been used here only in Section 6 to test the impact of assimilating the ASCAT data.

SIM describes soil moisture in three-layers: the near-surface (defined over the depth of bare soil evaporation), the root-zone soil moisture (defined over the depth of transpiration), and the deep-layer soil moisture (defined from the base of the root-zone to the base on the soil layer). The soil moisture in the *nth* layer is partitioned into the liquid water content, ω_n, and the solid water content $\omega_{I,n}$.

3 Methods

3.1 Processing the ASCAT soil moisture

Since scatterometer observations taken in the evening have been shown to produce less accurate soil moisture fields than early morning observations (Wagner et al., 1999, 2007), observations from the ascending (evening) and descending (morning) ASCAT overpasses have been considered separately in this report. MetOp takes only a few minutes to cross the SIM model domain, and approximately 100 minutes to complete a full orbit. All ASCAT data from each orbit were assumed to occur at the same time, which has been rounded to the nearest hour. The ASCAT data have been provided by TU-Wien on the 0.125º Discrete Global Grid, and it has been projected onto the SIM model grid, before being evaluated or assimilated. The projection is obtained by assigning each ASCAT observation to all SIM grid points within 0.15º, and then taking the mean of all observations assigned to each model grid. This method ensures that all SIM grids within an observed swath are assigned data, while retaining the resolution of the spatial features in the original ASCAT data.

Before the ASCAT data were projected onto the SIM grid, the data were screened to remove:

- Observations with an ASCAT Estimated Soil Moisture Error (ESME) greater than 20%, (equivalent to approximately 0.1 m^3m^{-3}) : The ESME is provided with the ASCAT SDS to provide a measure of the performance of the change-detection model in extracting the SDS from the backscatter observations for the given surface conditions. The ESME screening mostly removes observations at densely vegetated locations.
- Observations for which the ASCAT surface state flag indicates either a frozen surface, temporary surface water, or the presence of snow: The surface state flag gives a probability of each of these events, based on the historic model parameters at each location. Note that in Section 3.3 it is shown that the surface state flag does not effectively identify all instances of frozen surface conditions, and an additional check for frozen ground cover will subsequently be applied.

Once the data have been projected onto the SIM grid, an additional static mask is applied to remove:

- Urban regions, identified as having an urban fraction greater than 15% in the ECOCLIMAP database (Masson et al., 2003)
- Steep mountainous terrain, identified as having a topographic complexity flag (provided with the ASCAT data) greater than 15%
- Open water, based on a wetland fraction (provided with the ASCAT data) greater than 5%

3.2 Time series comparisons at the SMOSMANIA sites

In section 4, the ASCAT SDS have been evaluated by temporal comparison to in situ observations and SIM model simulations at the 12 SMOSMANIA sites. As described above, the ASCAT data have been projected onto the SIM grid, and the ASCAT and SIM time series for each SMOSMANIA site are taken from the surrounding SIM grid. For SIM, a once daily ω_1 time series has been constructed from the archived near-real time SIM ω_1 at the same time as each ASCAT observation. On days when ASCAT observations were not available, the SIM time series plots are filled in with the simulations at 9:00 UTC (descending pass) and 21:UTC (ascending pass). The in situ SMOSMANIA time series are constructed from the near-surface (5 cm) soil moisture observations at the same times as were used for SIM. Both the SIM and in situ soil moisture fields have been converted from a volumetric (m^3m^{-3}) soil

moisture (ω) to a SDS, equivalent to the metric observed by ASCAT, by normalizing the time series at each SMOSMANIA site by its range:

$$SDS = (\omega - \omega_{min}) / (\omega_{max} - \omega_{min}) \quad (1)$$

The minimum and maximum values for each time series are estimated from the 1st and 99th percentiles, respectively, to minimise the potential of using outliers as the upper/lower bound. Table 1 shows the minimum and maximum soil moisture bounds used to calculate the SDS at each site. Since there are significant representativity errors between soil moisture from in situ sensors and models, it is not surprising that there is little similarity between the range described by each data set: in particular the SMOSMANIA bounds are often wetter than those from the SIM, particularly at the dry end.

The SDS time series for SMOSMANIA, SIM, and ASCAT have been compared visually, and quantitatively by calculating the bias, Root Mean Square Difference (RMSD), absolute correlation, and anomaly correlation between them. The anomaly correlation is calculated by defining the anomalies as the difference from the 30-day (central) moving average. The significance of each of the estimated correlation values has been tested at the 1% level. For the absolute correlation the very high serial correlation in soil moisture time series reduces the number of independent data in the time series, introducing a bias in statistical inference (although not in the correlation estimate itself). Since soil moisture time series can be approximated by a first-order Markov processes (Vinnikov and Yeserkepova, 1991), the 'effective sample size' of Dawdy and Matalas (1964) has been used for significance testing the estimated correlations. The effective sample size, N_{eff}, is calculated using:

$$N_{eff} = N (1 - r_x r_y)/(1 + r_x r_y) \quad (2)$$

Where N is the sample size, and r_x and r_y are the lag-1 serial correlations of the two data sets being tested.

Table 1: Minimum and maximum soil moisture bounds (m^3m^{-3}) used to convert SMOSMANIA and SIM near-surface soil moisture to an SDS.

	SMOSMANIA		SIM	
Site	ω_{min}	ω_{max}	ω_{min}	ω_{max}
SBR	0.06	0.31	0.10	0.28
URG	0.13	0.58	0.12	0.36
CRD	0.08	0.29	0.11	0.34
PRG	0.18	0.44	0.15	0.43
CDM	0.20	0.47	0.13	0.41
LHS	0.17	0.46	0.14	0.42
SVN	0.12	0.47	0.10	0.37
MNT	0.16	0.53	0.12	0.38
SFL	0.13	0.38	0.11	0.40
MTM	0.14	0.30	0.10	0.34
LZC	0.05	0.34	0.08	0.31
NBN	0.11	0.37	0.09	0.33

3.3 The Simplified Extended Kalman Filter

In Section 6, the root-zone soil moisture in the SIM model (forced with the near-real time SAFRAN analyses) is analysed by assimilating the ASCAT surface degree of saturation observations using a Simplified Extended Kalman Filter (SEKF). The impact of the assimilation on the model skill is then tested by comparison to the in situ soil moisture observations from SMOSMANIA, and to archived fields from the SIM model forced with higher quality observations (from the delayed cut-off climatological chain).

The SEKF, as formulated by Mahfouf et al (2009) and Draper et al (2009) has been used for the assimilation. Since the ISBA model has no horizontal component, the SEKF is performed as an individual 1-D assimilation at each model grid. The Extended Kalman Filter equations for the i^{th} model state forecast and update for the i^{th} timestep, t_i are:

$$\mathbf{x}^b(t_i) = M_{i-1}\mathbf{x}^a(t_{i-1})$$

and

$$\mathbf{x}^a(t_i) = \mathbf{x}^b(t_i) + \mathbf{K}(\mathbf{y}_i^o - H(\mathbf{x}^b(t_i))$$

where **x** indicates the model state and **y** is the observation vector. The superscripts *a*, *b*, and *o* indicate the analysis, background, and observations, respectively. *M* is the nonlinear state forecast model, and, *H* is the nonlinear observation operator (mapping the model state into the observation state space). **K** is the Kalman gain, given by:

$$\mathbf{K}_i = \mathbf{P}^f(t_i)\mathbf{H}_i^T(\mathbf{H}_i\mathbf{P}^f(t_i)\mathbf{H}_i^T + \mathbf{R}_i)^{-1}$$

P and **R** are the covariance matrices of the model background and observation errors, respectively, and **H** is the linearization of *H*. As mentioned above, the three-layer version of ISBA used in SIM describes soil moisture as three variables: the near-surface soil moisture (ω_1), the root-zone soil moisture (ω_2), and the deep-layer soil moisture (ω_3). In these experiments the state update vector included ω_1 and ω_2, and the ASCAT observations were assumed to be the observation-equivalent of the model ω_1. An integration of the forecast model has been used as the observation operator, and *H* has been linearised by finite differences, following Seuffert et al (2004). The impact of ω_2 on ω_1 increases with time, and a 24-hour forecast length was chosen for the observation operator, as a compromise between a long enough forecast length that ω_2 has a reasonable impact on ω_1, and short enough forecast that it can be linearised without a significant loss of accuracy.

Finally, the defining feature of the EKF is that the background model error is also evolved through a series of model forecasts and updates:

$$\mathbf{P}^f(t_i) = \mathbf{M}_i\mathbf{P}^a(t_{i-1})\mathbf{M}_i^T + \mathbf{Q}(t_i)$$

and

$$\mathbf{P}^a(t_i) = (\mathbf{I} - \mathbf{K}_i\mathbf{H}_i)\mathbf{P}^f(t_i)$$

where **Q** is the error covariance matrix for the (additive) model forecast error, and **M** is the linearization of *M*, also obtained by finite differences. However, Draper et al (2009) found that for the EKF as it is described here, evolving **P** through time with the above two equations does not generate substantial differences in the analysed soil moisture, compared to the simplified form of Mahfouf et al

(2009), in which the same **P** matrix is used at the start of each assimilation cycle. Consequently, the simplified EKF has been used here, and the above two equations have been neglected.

The application of the SEKF will be further described in Section 6.1, including the selection of the model and observation error, and the bias correction applied to minimise the systematic differences between the soil moisture fields from the SIM and ASCAT.

3.4 Detecting frozen surface conditions in ASCAT observations

Previous studies have shown that occurrences of frozen surface conditions are not adequately identified by the SDS retrieval, resulting in anomalously low SDS values during frozen conditions, for both ERS (Pellarin et al, 2006) and ASCAT (Brocca et al., 2010a). This is demonstrated in Figure 2, which shows the ASCAT and SMOSMANIA SDS, with the ASCAT data plotted in blue where SIM has forecast non-zero frozen soil moisture, and in red otherwise. Since SIM is forced by a screen-level analysis its surface temperature simulations are thought to be reasonably accurate. This has been qualitatively confirmed by comparing the simulation of non-zero near-surface soil moisture against the observed soil temperature (at 5 cm) at the SMOSMANIA sites; note that the deeper layer

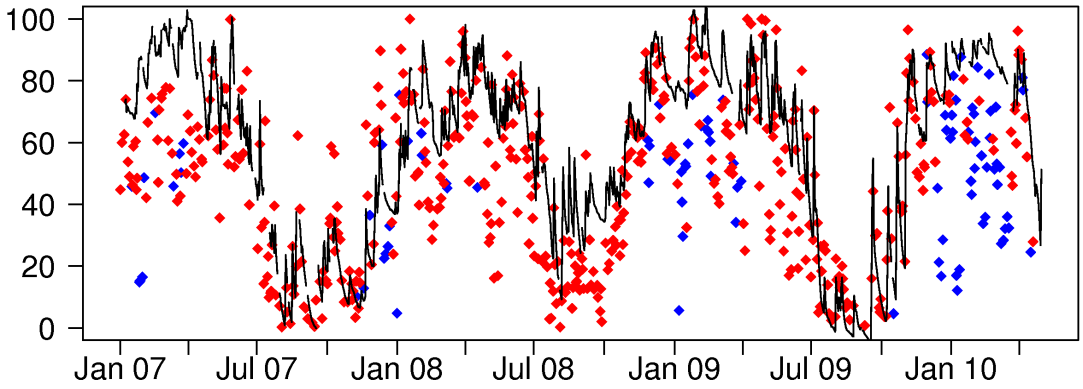

Figure 2. Surface degree of saturation at URG from SMOSMANIA in situ observations (black line), and descending overpass ASCAT observations (diamonds). Blue (red) diamonds indicate presence (absence) of frozen near-surface soil moisture in SIM model simulations.

observed by the SMOSMANIA sensors freezes less readily. There is a strong tendency in Figure 2 for the ASCAT observations to be anomalously low, compared to the SMOSMANIA observations and the preceding ASCAT observations, at times when SIM has forecast nonzero frozen near-surface soil moisture. This suggests that the probabilistic surface state flag used in the ASCAT retrieval is not sufficient to identify and remove the occurrence of frozen surface conditions. As noted by Pellarin et al. (2006) these anomalously low values are problematic for the retrieval of the root-zone soil moisture from SDS time series using the exponential filter, since the filtered time series has a long memory of these anomalously low erroneous observations (and the same would be true when assimilating the SDS into a more sophisticated model to retrieve root-zone soil moisture). Consequently, the ASCAT surface degree of saturation should be screened to remove frozen surface cover using ancillary data sources, before being used in an exponential filter or assimilation. Additionally, for the remainder of this report, a frozen surface mask has been applied to the ASCAT data, based on SIM forecasts of nonzero frozen soil moisture.

Figure 3 shows maps of the coverage of the SIM and ASCAT SDS for the descending ASCAT overpass, after this mask is applied to both data sets (note the locations in red with no ASCAT data, due to the previously discussed quality control). On average, SIM has forecast nonfrozen ω_1 on 71% of days during the three and a half year study period, while the mean coverage of the ASCAT SDS (at

only those locations where some data are available) is reduced from 35% to 26% of days by the frozen surface mask. Applying this mask has a positive impact on the statistics between the in situ and ASCAT soil moisture time series, for the example at the URG site plotted in Figure 2, the correlation is increased from 0.78 to 0.83.

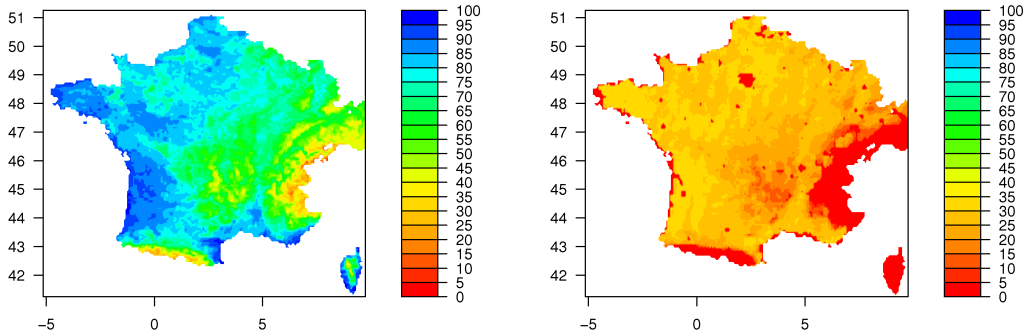

Figure 3. Coverage (% of days) of SIM ω_1 (left) and descending overpass ASCAT SDS (right) from January 2007 to May 2010.

4 Comparison to SMOSMANIA in situ observations and SIM model forecasts

This section presents an inter-comparison of the SDS from ASCAT observations, the archived near-real time SIM forecasts, and the in situ SMOSMANIA observations. The ASCAT data are considered separately for the ascending and descending overpasses, and the results from the updated ASCAT(ASCAT) retrieval algorithm are also compared to those from the older ASCAT(ERS) algorithm.

4.1 Descending overpass ASCAT observations

Plots comparing the SDS from the ASCAT descending pass, SMOSMANIA, and SIM at each of the SMOSMANIA sites are shown in Figure 4, and descriptive statistics for each time series are listed in Table 2. While the ASCAT time series have much more short term variability, the agreement between SMOSMANIA and ASCAT in Figure 4 is quite good: the timing of the seasonal cycle in the SMOSMANIA observations is well predicted by ASCAT, as are the sharp peaks associated with rain events. The exception is at the MTM site, where the ASCAT data does not have a clear seasonal cycle and has little agreement with the SMOSMANIA time series. The poor results at MTM are likely due to its location in hilly terrain (MTM is the highest of the SMOSMANIA stations). There were virtually no data available at this site for the previous ASCAT(ERS) data set (Albergel et al., 2009), presumably due to the failure of the retrieval algorithm in complex terrain (possibly in combination with dense vegetation cover in the surrounding region). With the higher resolution model parameters used by ASCAT(ASCAT), observations are now available at MTM, although they are not available for the neighbouring discrete global grid approximately 12.5 km further south.

Table 2. Number of observations (no.), mean, and standard deviation (stdev) of the SMOSMANIA, SIM, and ASCAT (descending overpass) SDS data sets from January 2007 to May 2010. All statistics except for the number of observations are calculated using only days in which all data sets are available.

Site	SMOSMANIA			SIM			ASCAT		
	no.	mean %	stdev %	no.	mean (bias) %	stdev %	no.	mean (bias) %	stdev %
SBR	973	33.3	23.0	1055	42.9 (9.6)	25.8	562	61.1 (27.8)	23.7
URG	946	56.8	28.0	1012	48.8 (-8.0)	27.1	471	46.9 (-9.9)	26.5
CRD	942	30.6	26.3	1069	46.6 (16.0)	26.8	554	52.9 (22.3)	25.0
PRG	913	45.6	27.2	981	51.0 (5.4)	27.2	457	43.0 (-2.6)	27.5
CDM	984	50.6	29.0	1047	49.2 (-1.4)	27.0	491	41.8 (-8.8)	27.8
LHS	918	48.7	30.2	975	49.0 (0.3)	28.8	478	41.1 (-7.6)	25.5
SVN	882	33.9	27.3	938	42.6 (8.6)	26.8	438	38.9 (5.0)	27.0
MNT	848	48.2	26.7	913	45.3 (-2.9)	27.3	440	37.7 (-10.5)	25.9
SFL	892	46.8	30.9	953	48.2 (1.4)	27.9	472	36.8 (-10.0)	25.8
MTM	1006	58.5	26.2	1036	36.1 (-22.4)	25.6	499	31.7 (-26.8)	16.9
LZC	983	31.2	25.2	1130	36.7 (5.5)	24.0	499	27.3 (3.9)	22.6
NBN	1085	37.4	28.4	1133	35.8 (-1.6)	22.4	451	23.3 (-14.1)	20.9

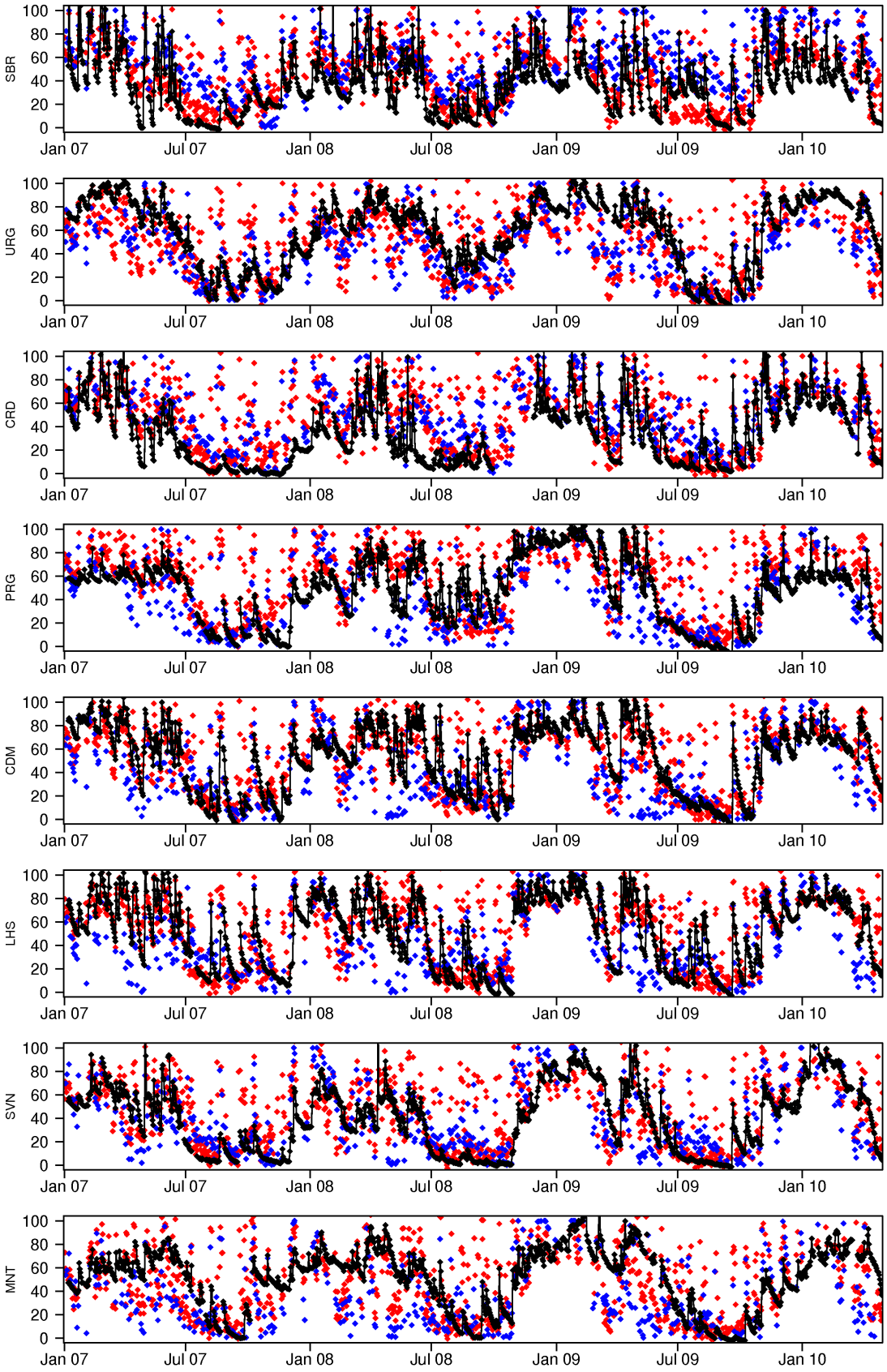
SBR
URG
CRD
PRG
CDM
LHS
SVN
MNT
0
20
40
60
80
100
Jan 07
Jul 07
Jan 08
Jul 08
Jan 09
Jul 09
Jan 10

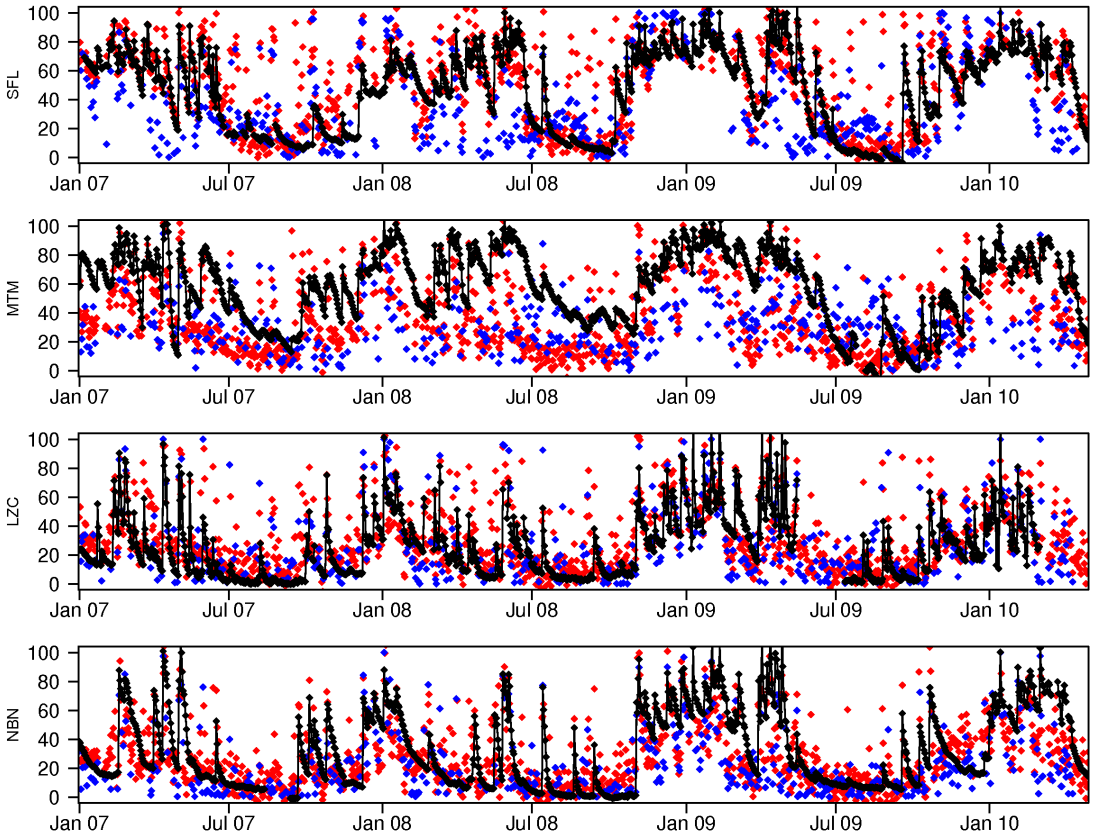

Figure 4. Time series of the surface degree of saturation (%) from SMOSMANIA (black), SIM (red), and ASCAT (blue) at each SMOSMANIA site.

There are significant differences between the absolute magnitude of the ASCAT and SIM SDS time series. In many instances the winter maxima from ASCAT are lower than those from SMOSMANIA, and there are also many anomalously low ASCAT observations during winter, suggesting that SIM may not have accurately detected all instances of frozen soil. Consequently, the bias between the ASCAT and SMOSMANIA observations in Table 2 is negative at most sites. Two significant exceptions are SBR and CRD, where ASCAT is consistently about 20% higher than the SMOSMANIA observations, resulting in large positive biases. The biases between the ASCAT and SMOSMANIA SDS contribute to the consistently large RMSD between them in Table 3, which ranges between 16.3% and 32.7%, with a mean of 24.3% (excluding MTM). This relatively large RMSD indicates a discrepancy between the absolute degree of saturation observed by ASCAT and SMOSMANIA, and while this could indicate errors in the ASCAT observations, it is as likely due to representativity errors between the (point based) in situ observations over a 5 cm soil layer and the (area-averaged) remotely sensed data over a 1 cm layer.

Time series of the surface degree of saturation time series calculated from the archived near-real time SIM forecasts are also plotted in Figure 4. In general, the SIM time series agree more closely with the absolute value of SMOSMANIA throughout the seasonal cycle than the ASCAT data does. Consequently, the biases for the SIM time series in Table 2 are smaller than those for ASCAT, resulting in smaller (although still substantial) RMSD in Table 3, with a mean across the sites of 21.9 % or 0.065 m^3m^{-3}. Of greater interest however, is that the SIM and ASCAT time series appear to be more similar to each other than either is to the SMOSMANIA data. Both SIM and ASCAT have more short term variability than the SMOSMANIA time series, and both diverge away from the SMOSMANIA time series in several instances: for example July 2007 at CRD, when ASCAT and SIM dry down more gradually than SMOSMANIA. In most instances these differences are consistent with the shallower depth of the ASCAT and SIM soil moisture values (both approximately 1 cm),

compared to the deeper layer observed by SMOSMANIA (5 cm). Note that while the depths of the ASCAT soil moisture observations and the SIM near-surface soil moisture are both typically quoted as being approximately 1 cm, both relate to soil moisture over a variable depth, and in fact have opposing dependencies on soil moisture. For the ASCAT observations, the penetration depth of the microwave signal increases as the soil dries, while for SIM ω_1 is defined over the depth of bare soil evaporation, which decreases as the soil dries. For SIM the decreasing depth of ω_1 will accelerate the rate of drying, which may explain some of the apparent noise in Figure 4, since the anomalously low SIM values often correspond to periods of drying in the SMOSMANIA observations.

Scatterplots comparing both the SIM and ASCAT surface degree of saturation to the SMOSMANIA data are shown in Figure 5, and statistics comparing all three data sets are listed in Table 3. The scatterplots show a reasonably linear relationship between SMOSMANIA and both ASCAT and SIM, and this is reflected by the consistently significant and generally high correlations in Table 3. Excluding MTM, the absolute correlations between the ASCAT and SMOSMANIA time series range

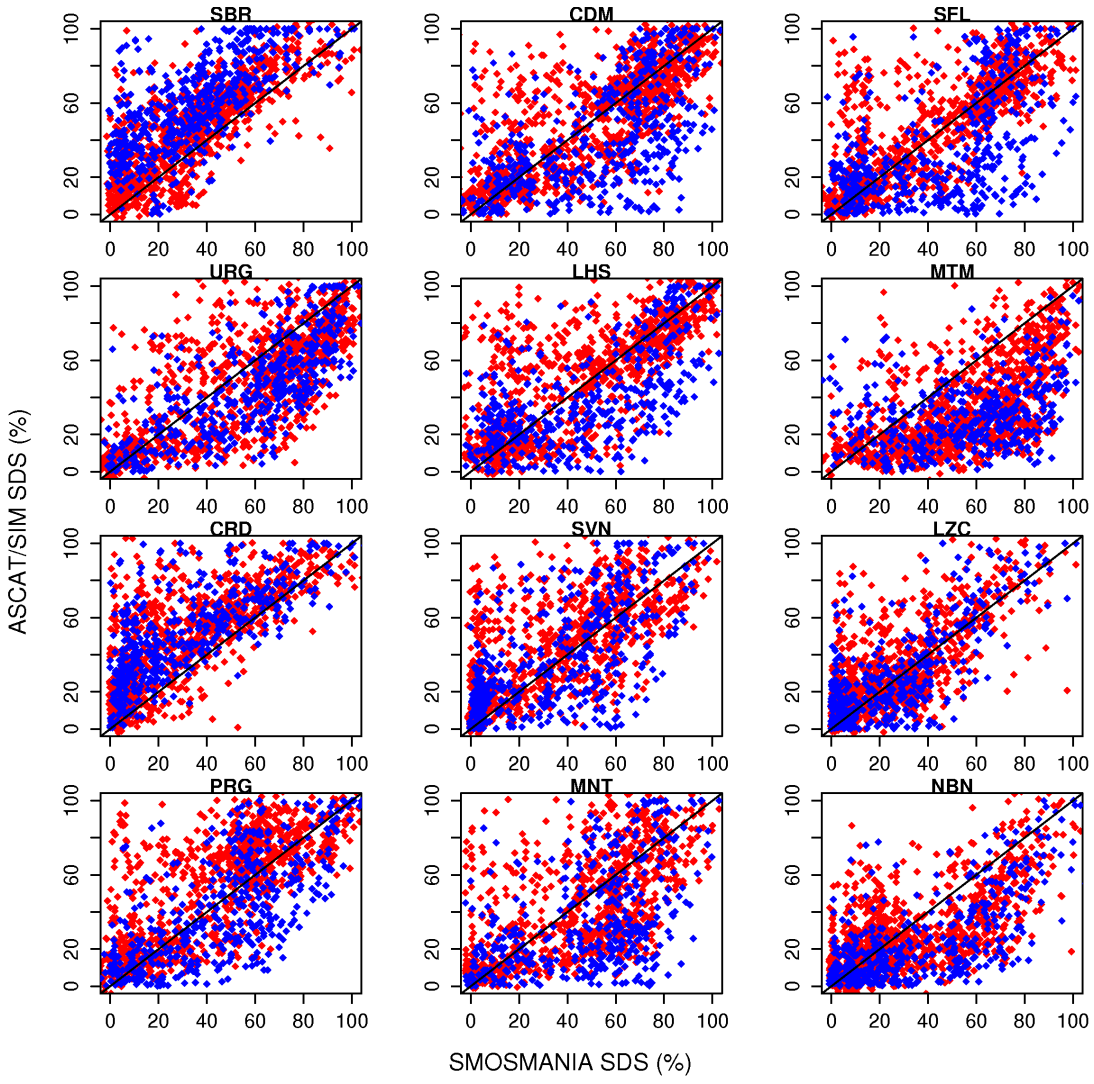

Figure 5. Scatterplots comparing the SIM (red) and ASCAT (blue) SDS to the SMOSMANIA SDS (all in %) at each SMOSMANIA site, from January 2007 to May 2010.

Table 3. Absolute correlation (r_{abs}), anomaly correlation (r_{anm}), and RMSD between combinations of the SMOSMANIA, SIM and ASCAT (descending overpass) SDS time series at each of the SMOSMANIA sites, from January 2007 to May 2010. All statistics are calculated using only days on which all data sets are available. For each statistic the best result is indicated in bold, and all correlations are significant at 1%.

Site	SIM / SMOSMANIA			ASCAT / SMOSMANIA			ASCAT / SIM		
	r_{abs}	r_{anm}	RMSD %	r_{abs}	r_{anm}	RMSD	r_{abs}	r_{anm}	RMSD %
SBR	**0.81**	**0.72**	**19.0**	0.73	0.65	31.2	0.74	0.71	25.5
URG	0.67	0.68	23.7	**0.83**	**0.74**	22.0	0.79	0.68	**17.5**
CRD	0.72	0.56	25.2	0.78	0.59	27.1	**0.84**	**0.71**	**16.2**
PRG	0.67	0.43	21.9	0.70	0.57	21.6	**0.78**	**0.72**	**19.8**
CDM	0.74	0.57	**19.6**	0.63	0.62	26.5	**0.75**	**0.76**	20.8
LHS	**0.70**	0.43	**22.4**	0.65	0.56	25.9	0.68	**0.72**	23.4
SVN	0.71	0.56	22.1	0.70	0.58	22.4	**0.77**	**0.72**	**18.7**
MNT	0.62	0.56	24.0	0.62	0.58	27.3	**0.71**	**0.66**	**21.7**
SFL	**0.73**	0.47	20.4	0.60	0.53	28.9	0.70	**0.68**	23.9
MTM	**0.61**	**0.54**	31.2	0.35	0.35	40.1	0.35	0.35	**25.5**
LZC	0.73	0.69	18.4	**0.78**	**0.78**	**16.4**	0.73	0.66	19.6
NBN	0.66	0.56	20.3	0.68	0.61	26.2	**0.75**	**0.68**	**19.7**

Table 4. Absolute correlation (r_{abs}), anomaly correlation (r_{anm}), and RMSD between combinations of the SMOSMANIA, SIM and ASCAT (ascending overpass) SDS time series at each of the SMOSMANIA sites, from January 2007 to May 2010. All statistics are calculated using only days on which all data sets are available. For each statistic the best result is indicated in bold, and all correlations are significant at 1%.

Site	SIM / SMOSMANIA			ASCAT / SMOSMANIA			ASCAT / SIM		
	r_{abs}	r_{anm}	RMSD %	r_{abs}	r_{anm}	RMSD %	r_{abs}	r_{anm}	RMSD %
SBR	**0.79**	**0.68**	**18.2**	0.69	0.56	29.9	0.68	0.59	25.4
URG	0.67	**0.70**	24.3	0.74	0.54	22.7	**0.75**	0.58	**19.1**
CRD	0.72	0.60	24.0	0.73	0.52	26.5	**0.77**	**0.61**	**18.8**
PRG	**0.71**	0.50	**22.3**	0.68	0.46	22.6	0.69	**0.53**	24.9
CDM	**0.75**	**0.62**	**19.9**	0.57	0.51	28.2	0.68	0.58	24.3
LHS	**0.73**	0.53	**21.2**	0.63	0.55	25.2	0.64	**0.65**	25.1
SVN	0.69	0.58	21.8	0.64	0.60	23.6	**0.71**	**0.64**	**20.9**
MNT	0.59	0.60	25.1	0.49	0.53	30.1	**0.71**	**0.62**	**22.3**
SFL	**0.81**	0.60	**17.7**	0.57	0.58	27.8	0.69	**0.68**	24.5
MTM	**0.58**	**0.56**	32.7	0.33	0.33	36.5	0.46	0.49	**23.3**
LZC	0.74	0.66	**17.7**	**0.76**	**0.74**	17.8	0.73	0.63	18.6
NBN	0.67	0.57	21.9	0.68	0.62	23.5	**0.73**	**0.66**	**17.0**

between 0.60 and 0.81, with a mean of 0.70, while the correlations between SIM and SMOSMANIA are similar, ranging between 0.62 and 0.81, with a mean of 0.71. At MTM the poor fit between the ASCAT and SMOSMANIA time series in Figure 4 results in a very low correlation of 0.35. Overall the absolute correlation to the SMOSMANIA observations is similar for ASCAT and SIM.

Since the correlation is heavily influenced by the agreement between the seasonal cycles of the time series, the anomaly correlation is also included in Table 3. For many applications, including data assimilation, the anomaly correlation gives a better metric of the value of the remotely sensed data. In

most instances the scatterplots of the anomalies (not shown) indicate a strong linear relationship between the SDS anomalies from SMOSMANIA and both ASCAT and SIM. For ASCAT the anomaly correlations with the SMOSMANIA data are significant at every site, with values ranging between 0.53 to 0.78 and a mean of 0.62, while for SIM the anomaly correlations with SMOSMANIA are again significant, although slightly lower, ranging from 0.43 to 0.72, with a mean of 0.57 (excluding MTM in both cases). ASCAT has higher correlation anomalies with the SMOSMANIA data than SIM at 10 out of 12 SMOSMANIA sites, suggesting that ASCAT might be a better predictor of short-term variability in the SMOSMANIA time series.

The best statistics at each site (between the different combinations of ASCAT, SIM, and SMOSMANIA) are indicated in bold in Table 3. Consistent with the earlier finding that the SIM and ASCAT time series have the best qualitative agreement, the best quantitative agreement at most of the sites is again between these two data sets. Excluding MTM the absolute correlations between ASCAT and SIM ranges between 0.68 and 0.84, with a mean of 0.75, and the anomaly correlations are almost as high, ranging between 0.66 and 0.86, with a mean of 0.70 (and all are significant). As with the time series in Figure 4, there are also similarities evident between SIM and ASCAT in the scatterplots in Figure 5. In particular, at several locations (CRD, SVN, MNT) the gradient for both SIM and ASCAT is steeper closer to zero than it is for wetter soils, which is consistent with the occurrence of accelerated soil drying close to the surface in dry conditions.

4.2 Ascending overpass ASCAT observations

Only the descending overpass ASCAT SDS have been presented above, in response to previous findings that the ascending overpass observations are less accurate. To test the accuracy of the ascending pass ASCAT observations, Table 4 shows the statistics describing the fit between the ascending overpass ASCAT SDS and the in situ and SIM time series at each of the SMOSMANIA sites. This is the same information that is listed in Table 3 for the descending overpass ASCAT data. The statistics in Table 4 indicate that the ascending ASCAT overpass can detect a useful surface soil moisture signal: all correlations and anomaly correlations are significant, with means (excluding MTM) of 0.71 and 0.62, respectively, for comparison to the SMOSMANIA time series, and 0.65 and 0.56, respectively, for the comparison to the SIM time series.

As expected, comparing the statistics in Tables 3 and 4 indicates that the ascending ASCAT observations are not as accurate as the descending overpass observations. For the SMOSMANIA time series, the descending ASCAT SDS time series have higher correlations at all sites, and the anomaly correlations are higher at all sites except two, while for the SIM time series, the descending ASCAT SDS has higher correlations and anomaly correlations at all sites except NBN. Additionally, the anomaly correlations between the ascending ASCAT data and SMOSMANIA are no longer consistently better than those between SIM and SMOSMANIA (as they were for the descending pass in Table 3), with ASCAT higher anomaly correlations at just 4 out of 12 sites. These results are consistent with those of Brocca et al (2010b), who also showed that the soil moisture observations from the ascending ASCAT overpass are reasonable, although less accurate than the descending overpass.

4.3 Estimating the SDS random errors

As noted above, there are substantial systematic differences between each of the SDS data sets, resulting in the relatively large RMSD in Tables 3 and 4. Additionally, these differences are as likely due to representativity errors between the different data sets than to errors in the individual data sets, none of which can be assumed to represent the truth. Hence, the root mean square error between each data set and the unknown true soil moisture has also been estimated, based on an additive error model that accounts for constant bias and random error components (note the distinction between the root mean square error calculated here, and the root mean square difference presented earlier). For

example, the observed ASCAT SDS is written as the sum of the true (unknown) value, SDS_{TRUE}, a long term bias ($b_{ASCAT} = <SDS_{ASCAT} - SDS_{TRUE}>$, where <.> indicates the expectation), and a random error of zero mean, σ_{ASCAT}:

$$SDS_{ASCAT}=SDS_{TRUE} + b_{ASCAT} + \sigma_{ASCAT} \quad (3)$$

At each SMOSMANIA site the standard deviation of the three SDS data sets is similar, suggesting that this additive error model is a reasonable approximation (rather than an error model including a multiplicative component, such as that used by Scipal et al, 2008). Since the three soil moisture estimates used here are entirely independent, it can be assumed that their random errors are uncorrelated, and the RMSD between each pair of data set can be written:

$$\begin{aligned} <(SDS_{SIM} - SDS_{SMOSMANIA})^2> &= (b_{SIM} - b_{SMOSMANIA})^2 + <\sigma^2_{SIM}> + <\sigma^2_{SMOSMANIA}> \quad (4)\\ <(SDS_{ASCAT} - SDS_{SMOSMANIA})^2> &= (b_{ASCAT} - b_{SMOSMANIA})^2 + <\sigma^2_{ASCAT}> + <\sigma^2_{SMOSMANIA}> \\ <(SDS_{ASCAT} - SDS_{SIM})^2> &= (b_{ASCAT} - b_{SIM})^2 + <\sigma^2_{ASCAT}> + <\sigma^2_{SIM}> \end{aligned}$$

The difference between the biases from each pair of data sets is equivalent to the bias between those data sets, which can be obtained from the mean values in Table 2. If this is then combined with the pair-wise RMSD between the data sets from Table 3, the variance of the random errors can be obtained by rearranging the above three equations (note that the bias between each data set and the truth is not explicitly determined with this method). There is significant variability across the SMOSMANIA sites in the biases between the different SDS data sets in Table 2, and hence the error model in equation 3 has been applied separately at each site. The σ obtained with this method are an estimate of the root mean square of the random error between each data set and an assumed 'true' SDS, based on the assumption that a single truth applies to all three SDS data sets. While, this assumption is clearly broken by the representativity errors between the three data sets, the σ are thought to provide a better estimate of the actual errors than can be obtained by comparing the data sets pair-wise (and for example, estimating the errors in remotely sensed soil moisture by direct comparison to in situ data, since this effectively assigns all representativity error to the remotely sensed data).

The root mean square of the random errors estimated at each site are given in Table 5, separately for the ascending and descending ASCAT overpasses. For the descending overpass, the vales for ASCAT vary between 5.2 and 17.8%, with a mean of 12.5%, while the values for SIM are very slightly larger, with a range of 9.7 to 16.6%, and a mean of 13.0% (and ASCAT has the lowest σ at 6 out of 11 sites, while SIM has the lowest at four sites). If these error estimates are converted into volumetric soil moisture, based on the range of the SMOSMANIA soil moisture at each site (see Table 1), the root mean square of the random error averaged across the sites is 0.036 m^3m^{-3} for ASCAT and 0.039 m^3m^{-3}

Table 5. Root mean square error for each SDS data set (%), estimated using data from January 2007 to May 2010. For each overpass the lowest result is indicated in bold.

	Descending pass			Ascending pass		
Site	ASCAT	SIM	SMOSM.	ASCAT	SIM	SMOSM.
SBR	13.86	11.27	**10.10**	15.83	12.67	**10.49**
URG	**5.22**	16.56	14.91	**11.09**	15.39	16.13
CRD	**7.52**	12.89	15.23	**11.75**	13.59	14.58
PRG	**11.83**	13.68	17.42	16.39	**14.84**	15.00
CDM	16.84	**9.69**	17.73	20.13	**10.65**	16.70
LHS	16.32	**14.83**	17.21	18.55	**14.6**	15.34
SVN	13.39	**12.57**	16.18	16.25	**13.04**	16.88
MNT	**13.64**	15.05	18.22	17.68	**12.03**	21.29
SFL	17.82	**11.03**	18.72	21.34	**7.61**	15.93
MTM	19.75	**15.63**	16.52	18.69	**13.81**	18.90
LZC	**10.61**	13.47	11.79	13.25	12.97	**11.72**
NBN	**10.06**	11.48	18.18	**11.39**	11.81	17.23

for SIM. For ASCAT this is within the 0.04–0.05 m^3m^{-3} target accuracy for soil moisture remote sensing missions (Kerr et al., 2001; Walker and Houser 2004). The estimated root mean square random error for the descending pass SMOSMANIA are consistently larger, with a range of 10.1 to 18.7 %, and a mean of 16.0% (0.047 m^3m^{-3}). The larger values obtained for SMOSMANIA do not necessarily indicate inaccuracies in that data set, since the 'truth' against which these errors are measured will be more strongly influenced by the similar soil moisture definitions of ASCAT and SIM, than by the in situ SDS observations over a deeper soil moisture layer from SMOSMANIA.

For the ascending pass, the errors for SIM and SMOSMANIA are similar to the descending overpass, while ASCAT has consistently larger random errors, with a mean root mean square random error of 0.046 m^3m^{-3} across the SMOSMANIA sites. At most sites the SIM and SMOSMANIA estimated root mean square error is within 1-2 % of the value for the descending pass, giving similar mean volumetric root mean square errors of 0.037 m^3m^{-3} and 0.046 m^3m^{-3}, respectively. This similarity between the estimated errors for each overpass from both SIM and SMOSMANIA, despite the poorer performance of ASCAT, supports the choice of error model used in these calculations (since the SIM and SMOSMANIA errors are not expected to show a strong diurnal cycle).

4.4 Comparison to ASCAT retrieval algorithm based on ERS model parameters

The impact of updating the ASCAT retrieval method to use model parameters calculated from ASCAT observations, rather than older ERS-derived parameters is examined here (using the descending pass ASCAT data only). Albergel et al. (2010) compared ASCAT(ERS) SDS to the SMOSMANIA observations for 2007 to 2008, and this comparison is repeated here with the ASCAT(ASCAT) SDS. The methods used by Albergel et al. (2010) to process the ASCAT SDS and calculate statistics of fit to the SMOSMANIA data differ slightly from those applied earlier in this report, and so for consistency the methods of Albergel et al. (2010) (and Albergel et al. (2009)) are adopted in this Section. The main differences are:

- ASCAT data from the nearest Discrete Global Grid point are used
- ASCAT observations of frozen surface conditions have not been screened with ancillary data
- The SMOSMANIA data are a daily average
- To calculate the SMOSMANIA SDS the minimum and maximum of the time series are calculated using the inner-most 95% of the data, estimated using the mean and standard deviation (i.e., assuming normality), and the outer-most 5 % of the data are discarded
- The anomalies are calculated using a five week moving average window, and are scaled by both the mean and standard deviation within that window

As noted in Section 4.1 there are no data available at MTM for ASCAT(ERS), and while there are data available from ASCAT(ASCAT) it is of poor quality. At all other SMOSMANIA sites the coverage of the two data sets is similar.

Figure 6 shows a typical example comparing the two ASCAT SDS retrievals to the SMOSMANIA data, in this case at URG. The ASCAT(ASCAT) time series has a better visual fit to the SMOSMANIA data than the ASCAT(ERS) time series, and in particular it captures the full range of the seasonal cycle much more accurately. In contrast, the ASCAT(ERS) time series has a damped seasonal cycle with insufficient drying in summer, compared to the SMOSMANIA data. Figure 7 shows a scatterplot of the ASCAT(ASCAT) and ASCAT(ERS) SDS at URG. It shows that for ASCAT(ASCAT) above about 50%, the gradient of the plotted data is close to one (although shifted to the left of the one-to-one line), while for lower values the gradient flattens out, indicating that ASCAT(ERS) has a reduced sensitivity to changes in ASCAT(ASCAT). Consequently the statistics describing the temporal association between the SMOSMANIA data at URG in Table 6 give better results for ASCAT(ASCAT), with the correlation (anomaly correlation) increasing from 0.64 (0.39) to 0.73 (0.43). This result is repeated across all of the SMOSMANIA sites, with the ASCAT(ASCAT)

time series consistently showing an enhanced dynamic range in dry conditions, resulting in consistently more negative biases (at all sites but one) for ASCAT(ASCAT) than for ASCAT(ERS). This does not in general improve the biases, nor consequently the RMSD (which is improved at just 5 out of 12 sites). However, the correlation is increased at 9 out of 11 sites, from a range (excluding MTM) of 0.47 to 0.71 with a mean of 0.59 for ASCAT(ERS), to a range of 0.50 to 0.73, with a mean of 0.63 for ASCAT(ERS). The anomaly correlations increase by a larger margin, from a range of 0.18 to 0.71 with a mean of 0.37 for ASCAT(ERS), to a range of 0.43 to 0.63 with a mean of 0.48 for ASCAT(ERS). The large improvement in the anomaly correlation at NBN (from 0.18 to 0.45) is most likely associated with the increased resolution of the ASCAT(ASCAT) model parameters, since this station is within 15 km of the coast.

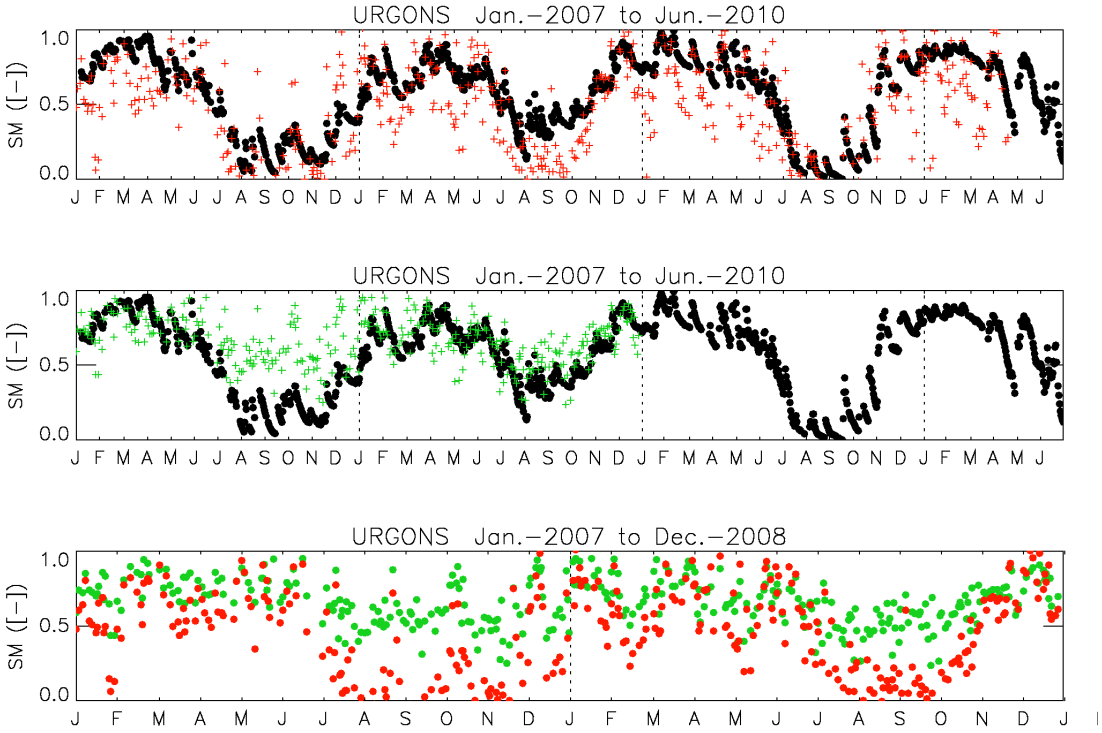

Figure 6. Time series of surface degree of saturation (scaled from 0 to 1) from ASCAT(ASCAT) (red), ASCAT(ERS) (green) and SMOSMANIA (black).

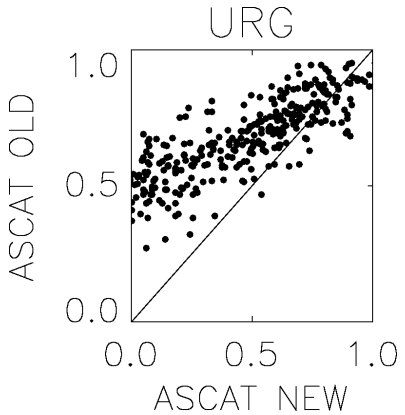

Figure 7. Scatterplot comparing the surface degree of saturation (scaled 0 to 1) from ASCAT(ASCAT) (new), ASCAT(ERS) (old) over 2007-2008.

Table 6. Absolute correlation (r_{abs}), anomaly correlation (r_{anm}), and RMSD comparing each of ASCAT(ASCAT) and ASCAT(ERS) SDS time series to the SMOSMANIA data for 2007 - 2008. For each statistic the best result is indicated in bold.

Site	ASCAT(ERS)				ASCAT(ASCAT)			
	r_{abs}	r_{anm}	bias	RMSD	r_{abs}	r_{anm}	bias	RMSD
SBR	0.71	0.55	19.2	22.9	**0.73**	**0.63**	**17.2**	**23.2**
URG	0.64	0.39	11.5	22.9	**0.73**	**0.43**	**-9.7**	**20.5**
CRD	0.63	0.38	32.9	35.7	**0.66**	**0.48**	**24.5**	**30.6**
PRG	0.59	0.36	**5.1**	20.9	**0.71**	**0.49**	-5.3	**20.8**
CDM	0.63	0.39	**-3.3**	**19.5**	**0.65**	**0.49**	-7.8	22.7
LHS	**0.62**	0.37	**-4.0**	**21.7**	0.57	**0.50**	-5.4	24.2
SVN	0.60	0.29	22.0	0.278	**0.64**	**0.42**	**19.6**	**28.2**
MNT	0.47	0.32	**-3.1**	**21.9**	**0.50**	**0.48**	-3.8	23.4
SFL	**0.51**	0.35	**5.1**	**24.5**	0.47	**0.41**	-6.0	26.7
MTM	-	-	-	-	0.26	0.17	-17.6	31.1
LZC	0.61	0.48	**12.1**	**20.1**	**0.70**	**0.48**	20.2	25.4
NBN	0.54	0.18	**5.2**	**21.1**	**0.56**	**0.45**	15.5	23.5

5 Comparison of SIM and ASCAT SDS over France

In Section 4.1 it was shown that there is a strong agreement between the near-surface soil moisture from near-real time SIM forecasts and from ASCAT observations. This confirms that these two data sets are observing/modeling similar soil moisture processes, and strongly suggesting that both are reasonably accurate at the SMOSMANIA sites. In this section, this comparison has been extended across the entire SIM domain, to test whether this result can be genaralised.

While the comparison in Section 4 was based on archived SIM forecasts, in this section (and in Section 6) the reported SIM forecasts have been generated by running the ISBA model with archived near-real time SAFRAN analyses (which yielded very slightly different results from the archived near real time SIM forecasts).

5.1 Temporal correlation

Figure 8 show maps of the correlation and anomaly correlation between the SIM ω_1 and ASCAT SDS over France. The strong agreement between the SIM and ASCAT near-surface soil moisture at the SMOSMANIA sites is repeated across France, and both the correlation and anomaly correlation are consistently high in Figure 8. For the correlation, the mean value across France was 0.69, and 87% of the SIM model grids had a value greater than 0.6, while for the anomaly correlation the mean was 0.62, and 77% of grids had a value greater than 0.6. The estimated correlations (anomaly correlations) were significant at a 1% level at all except 48 (43) grids, most of which were associated with infrequent ASCAT observations. The correlation and anomaly correlation maps have similar spatial patterns, in terms of the regions of high and low values. Both have several small regions with low correlations (<0.3), with a handful (less than 10 grids out of 14317 land points in SIM) of isolated instances of negative correlations (not shown in Figure 8). These reduced correlations all occur in mountainous regions adjacent to regions in which the ASCAT data have been screened out, suggesting that the low correlations are associated with ASCAT errors, and that the parameters used to mask the ASCAT data should be slightly expanded.

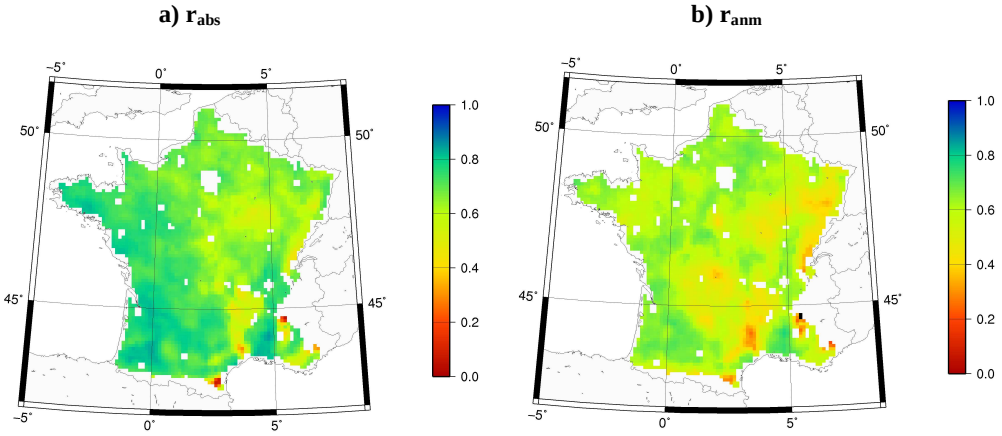

Figure 8. Maps of a) absolute correlation and b) anomaly correlation (right) between SIM ω_1 and ASCAT SDS from January 2007 to May 2010.

5.2 Absolute values

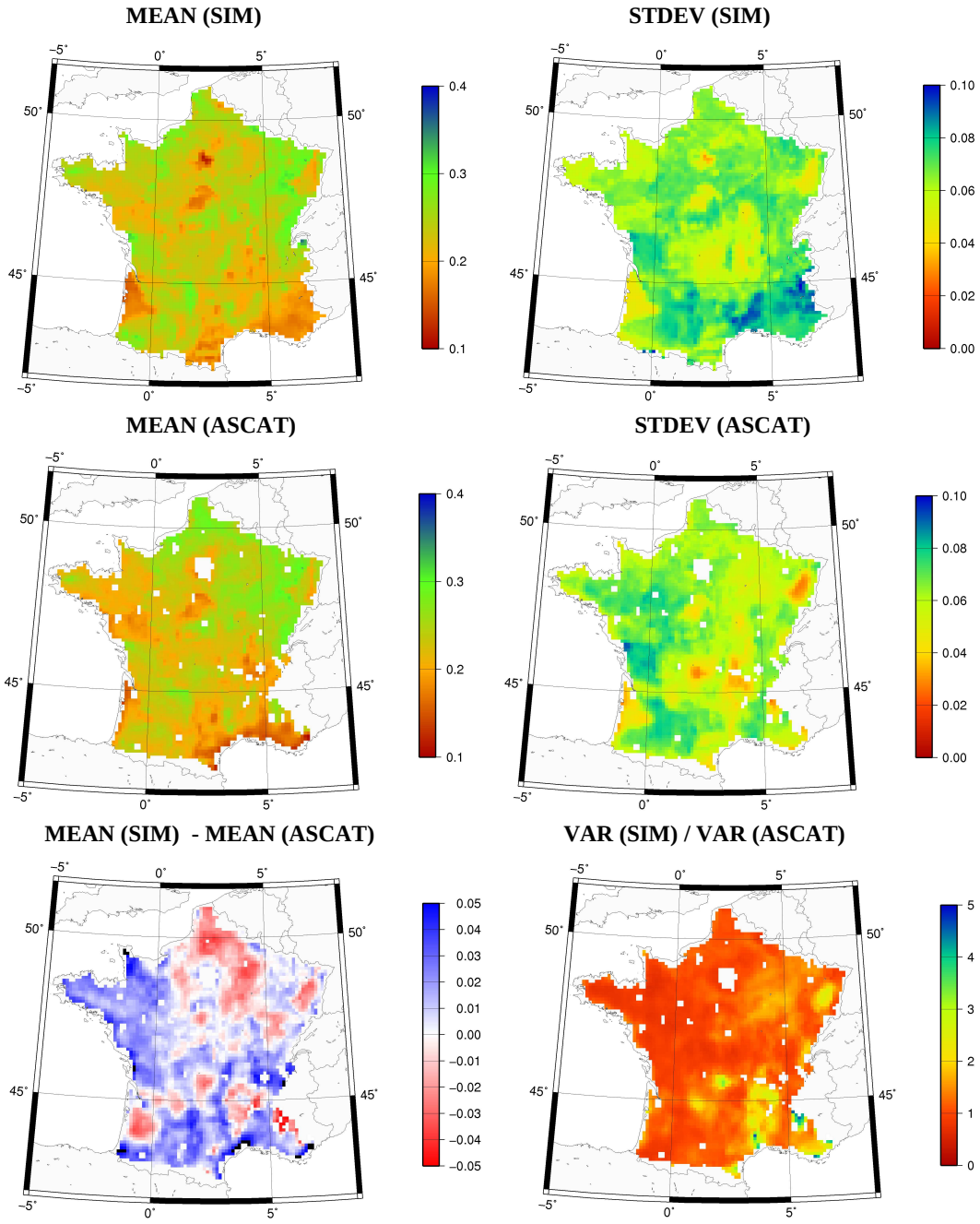

Figure 9. Maps of the mean (left) and standard deviation (right) of the near-surface soil moisture (m^3m^{-3}) from January 2007 to May 2010, from SIM (left) and ASCAT (right). The third row shows the difference in the mean (left) and the ratio of the variances (right) between SIM and ASCAT.

To examine the absolute differences between the two soil moisture data sets, Figure 9 compares maps of the mean and standard deviation of the near-surface soil moisture from SIM and ASCAT, with the ASCAT SDS converted to a volumetric soil moisture, based on the SIM climatology and equation 1. The strong agreement between the mean soil moisture from SIM and ASCAT, and in particular the similarity in their fine scale variability, arises from the use of SIM parameters in the conversion of the ASCAT SDS to a volumetric soil moisture. Maps of the ASCAT SDS (not shown) have much coarser

resolution of features, although the large-scale patterns of wetter and drier soils are similar to those in the mean soil moisture from SIM. The mean and standard deviation of the entire ASCAT soil moisture data set are 0.229 and 0.0701 m^3m^{-3}, respectively, already very close to the values of 0.236 and 0.0726 m^3m^{-3} for SIM. ASCAT indicates a drier near-surface soil layer across most of France, with the exceptions being in the northeast (in the Champagne-Picardie regions), and several other small regions throughout France, most of which are forested. The differences in the standard deviation from ASCAT and SIM are more marked, and in particular SIM has a region of strong variability in the southeast that is absent from ASCAT. Additionally, several isolated regions stand out as having an anomalously high ratio of variances between ASCAT and SIM, and comparison to Figure 8 shows that these locations are associated with relatively low anomaly correlation, suggesting that one data set may be inaccurate at these locations.

6 Assimilation Experiments

In this section the ASCAT SDS data are assimilated into the SIM model, using the SEKF described in Section 3.3, to test whether this will improve the model simulated surface states and moisture fluxes. The impact of assimilating the ASCAT SDS has been assessed principally by comparison to output from the SIM model forced with higher quality forcing generated from the delayed cut-off SAFRAN analysis (referred to as SIM_DEL). In the SIM simulations conducted here (referred to as SIM_NRT), lower quality near-real time SAFRAN output has been used to force ISBA. If the ASCAT observations can accurately detect temporal changes in near-surface soil moisture, then assimilating these observations (referred to as SIM_ASCAT) should draw the model towards SIM_DEL, although the success of the assimilation will also depend on the suitability of the assimilation approach, and the extent to which errors in the model ω_1 are coupled to errors in other variables.

Following the findings from Section 4.2, only the descending overpass ASCAT SDS data have been assimilated, and the observations of frozen surface conditions have been excluded by discarding the ASCAT data if SIM has simulated non-zero ω_{I1} during the current assimilation cycle.

6.1 Details of the SEKF assimilation

6.1.1 Bias-correcting the ASCAT observations

As was demonstrated in Figure 9, there are substantial systematic differences between modeled and observed near-surface soil moisture. These systematic differences have been reduced prior to assimilating the ASCAT SDS, by correcting the ASCAT data to the model climatology using the CDF-matching technique of Reichle and Koster (2004). The ASCAT SDS data have been normalised to have the same CDF as the SIM_NRT ω_1 forecasts. The CDF-matching was performed using the longest available record length, from January 2007 to May 2010.

The CDF-matching was very effective at removing the (already small) differences in the mean and standard deviation of the ASCAT and SIM soil moisture, and the resulting maps of the mean and standard deviation of the CDF-matched ASCAT soil moisture (not shown) are very similar to the maps for SIM in Figure 9, while the mean and standard deviation data for the full data record are the same as those quoted above in Section 4.5 for SIM_NRT.

6.1.2 The SEKF error covariances

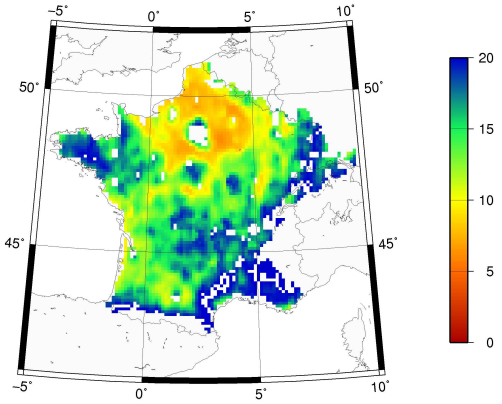

Figure 10. Maximum estimated ASCAT SDS error (in units of percentage of saturation), from January 2007 to May 2010 (values above 20 have been masked).

A major hurdle to the assimilation of novel near-surface soil moisture observations is the specification of accurate observation and model errors. Consequently, an estimate of the error in each observation is provided together with the ASCAT SDS. To test whether the provided error estimates can detect discrepancies between ASCAT and SIM (which may indicate errors in ASCAT), the ASCAT error estimates have been compared to the correlation between ASCAT and SIM. The maximum expected soil moisture error from January 2007 to May 2010 is shown in Figure 10. This map shows a reasonably strong correspondence to maps of the vegetation cover used in SIM (not shown), with greater errors occurring where vegetation cover is dense, and/or broadleaf trees are present. The expected negative relationship between the estimated error and the correlations (particularly the anomaly correlation) occurs in some regions (e.g., Massif Central), although this relationship is not consistent (e.g., Brittany). This weak relationship is shown more clearly in Figure 11, which shows a scatterplot of the maximum estimated error (across the data record) and the anomaly correlation. For all error values, the anomaly correlations occur most densely around 0.7, however as the error increases there are more occurrences of lower anomaly correlations, usually between 0.4 and 0.7. This suggests that the error estimates provided with the ASCAT SDS have some skill in detecting errors in the ASCAT soil moisture (note that the anomaly correlation will be reduced by errors in both ASCAT and SIM). Consequently, these error estimates have been used to define the observation errors for the SEKF assimilation on the ASCAT SDS.

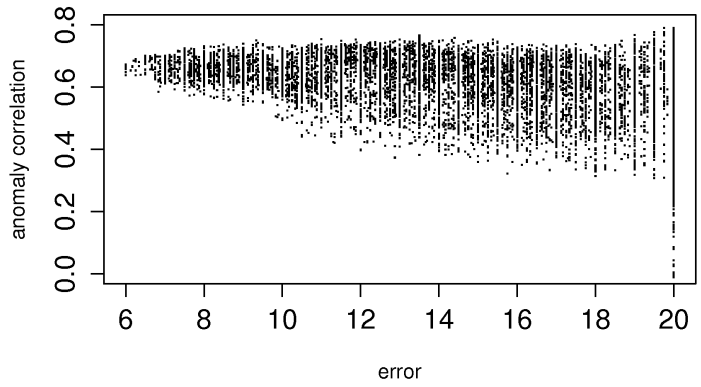

Figure 11. Scatterplot of the maximum ASCAT estimated soil moisture error vs. anomaly correlation between SIM ω_1 and ASCAT SDS, from January 2007 to May 2010.

The error estimates provided with ASCAT are in units of percentage of soil moisture at saturation (and are relative to the ASCAT soil moisture climatology), and they have been linearly rescaled to be consistent with the model soil moisture, by preserving the ratio between the original SDS and ASCAT error estimate at each grid. The original ASCAT SDS error estimates ranged between 3.5 and 20% (since all observations with an error greater than 20% have been screened out), with a median value of 9.0%. The rescaled error estimates ranged between 0.02 and 0.20 m^3m^{-3}, with a median value of 0.05 m^3m^{-3} (the very large values result from instances where the ASCAT estimated error was much larger than the ASCAT SDS; these values will effectively preclude the corresponding SDS from being assimilated). This median value is consistent with errors typically expected for remotely sensed soil moisture (e.g., Rüdiger et al, 2008), and is slightly higher than the root mean square error of 0.04 m^3m^{-3} estimated in Section 4.3.

For the background model errors, the error covariance matrix was assumed to be diagonal and the error variances were specified as a fraction of the soil moisture range at each grid point (defined by the difference between the field capacity (ω_{fc}) and the wilting point (ω_w)), following Mahfouf et al (2009). Since the SIM ω_1 and ASCAT SDS has similar accuracy in detecting temporal variability in near-surface soil moisture in Section, the background error standard deviation for ω_1 was set at 0.5x(ω_{fc} –

ω_w), giving a ω_1 error standard deviation close to 0.04 m^3m^{-3} across the domain, slightly less than the median value quoted above for the ASCAT observation error.

For ω_2, the background errors will be much lower, since the variability is lower and the soil moisture is less susceptible to errors in the atmospheric forcing. The SMOSMANIA observations do not span a sufficient depth to be sensibly compared to the SIM ω_2 forecasts, however several previous studies have evaluated ISBA forecast soil moisture against in situ observations throughout France. The root mean square error estimates from these studies span a range of values, with the ratio between the ω_1 errors (e_1) and ω_2 errors (e_2) varying from 0.2 for Calvet and Noilhan (2000) (e_1= 0.06, e_2= 0.015 m^3m^{-3}), to 0.4 for Sabater et al (2007) (e_1= 0.07, e_2 = 0.03 m^3m^{-3}), and 0.6 from Angueala et al (2008) (e_1 = 0.08, e_2=0.05 m^3m^{-3}), giving a mean ratio of 0.4. Additionally, the RMSD between SIM_DEL and SIM_NRT for the 3.5 year experimental period was 0.032 m^3m^{-3} for ω_1 and 0.014 for ω_2 m^3m^{-3}, giving the same ratio of 0.4 as was obtained above. Consequently, the ω_2 model background error standard deviation was specified to be 0.4 times the square root of the ω_1 error, or 0.2x($\omega_{fc} - \omega_w$).

6.2 Impact of assimilating the ASCAT SDS

The results of assimilating the ASCAT SDS are presented in this section. The results are first examined by considering individual time series at each of the SMOSMANIA sites. As was stated previously, the assimilation is principally assessed by comparison to the SIM_DEL simulations. The focus is on the impact on the root-zone soil moisture (ω_2), since the near-surface soil moisture (ω_1) has such a short memory. Additionally, the impact of the assimilation on the modeled surface water balance and river discharge is also tested.

6.2.1 Results at the SMOSMANIA sites

Figures 12 and 13 compare the time series of SIM_DEL, SIM_NRT, and SIM_ASCAT at each of the SMOSMANIA sites, for ω_1 and ω_2, respectively. Additionally, Tables 7 and 8 present the statistics of fit at each site between the SIM_DEL soil moisture, and each of SIM_NRT and SIM_ASCAT for the last three years of the experiment. For both soil moisture layers the SIM_DEL and SIM_NRT time series have very similar temporal behaviour, in that the timing of both the seasonal cycle and the response to individual precipitation events is very similar. Consequently the correlation and anomaly correlation statistics between SIM_DEL and SIM_NRT in Tables 7 and 8 are consistently very high (above 0.9 in all cases, and above 0.95 in most cases). However, for ω_2 there are periods spanning several months during which the SIM_NRT time series develop a clear bias relative to SIM_DEL. These biases have a tendency to be negative, and at all sites except LHS and SFL there was a net negative bias in Table 8, with a mean of -9.9 mm. The ω_1 time series are extremely noisy (even after a 10-day moving average filter was applied for the plot), and it is difficult to discern differences between the different time series, however the statistics in Table 7 indicate that the ω_1 SIM_NRT time series also have a tendency to be biased low, with substantial negative biases at each site (ranging between 10-50% of the standard deviation of SIM_DEL ω_1 time series), giving a mean bias of –0.0012 mm.

In most instances assimilating the ASCAT observations had no impact, or a slightly negative impact, on the correlations between the simulated soil moisture and SIM_DEL. This might not necessarily be due to the assimilation having had a detrimental impact on the model soil moisture, since the correlations between SIM_DEL and SIM_NRT were already very high, making it very difficult for the assimilation to add an additional source of variability to the model soil moisture without reducing the correlations. This is particularly the case since there will often be a delay between the introduction of an error to SIM_NRT, and the availability of the next ASCAT observation. The one exception to the small impact on the correlation statistics was at SBR, where the assimilation has reduced both r_{abs} and r_{anm} by a much larger amount (close to 0.1). Reference to the ω_2 time series in Figure 13 shows that this is caused by the assimilation having degraded the time series (relative to SIM_DEL) by incorrectly removing moisture in late 2007 and 2008, and then adding too much moisture in late 2009

(for both ω_1 and ω_2). The negative impact of the assimilation at SBR is also reflected in the relatively high RMSD for ω_2 in Table 8.

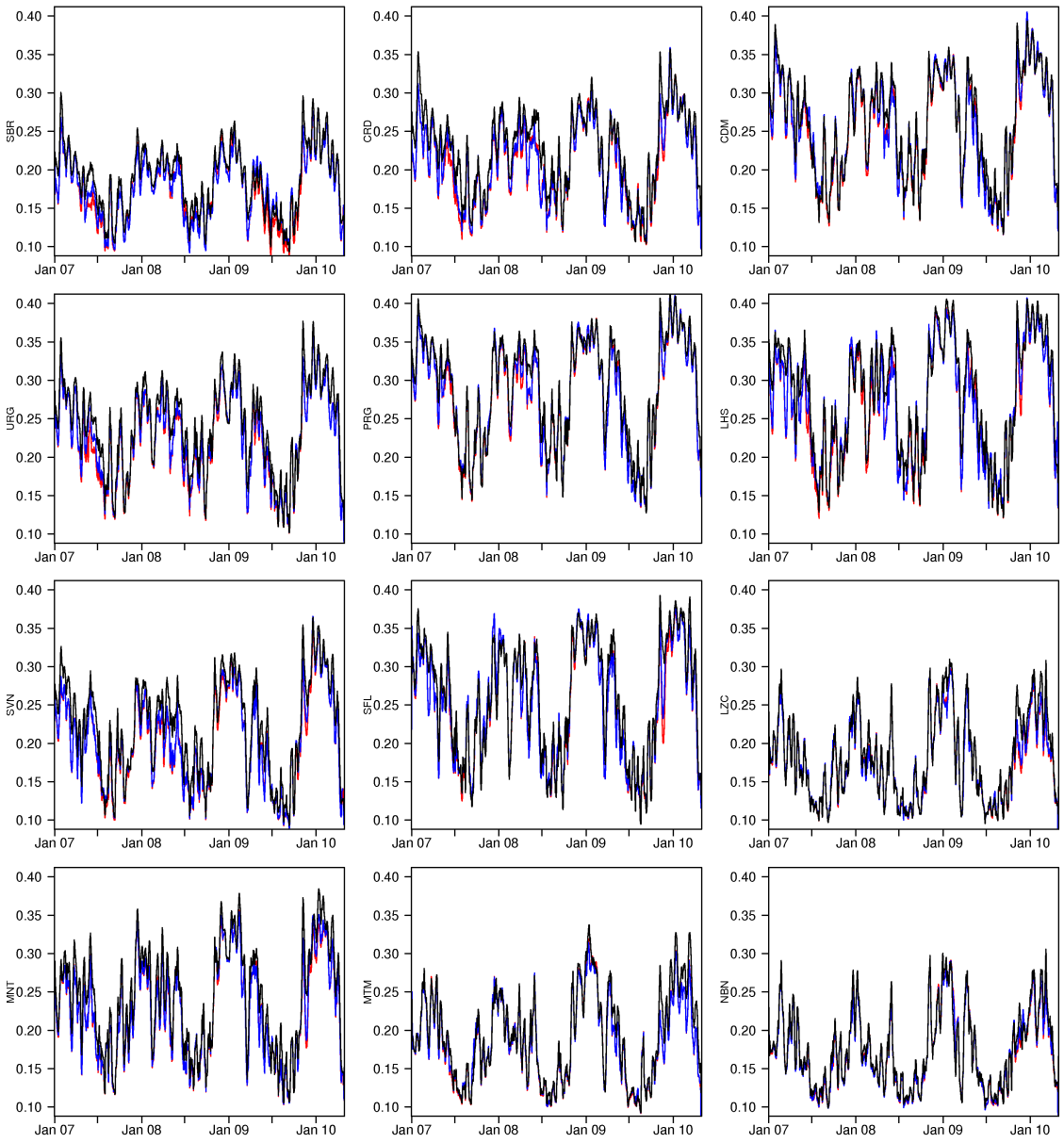

Figure 12. Time series of the ten-day moving average of the simulated ω_1 (m^3m^{-3}) at each of the SMOSMANIA sites, from SIM_DEL (black), SIM_NRT (red), and SIM_ASCAT (blue).

For ω_1, the assimilation consistently reduced the bias and RMSD, although by a very modest amount. The negative bias was reduced at all sites, reducing the mean from -0.0012 to -0.0010 mm. The RMSD was either unchanged (to two significant figures) or reduced, reducing the mean value across the sites from 0.0025 to 0.0024 mm. The impact of the assimilation on ω_2 is more substantial, but less consistent. At all sites the assimilation added net moisture to ω_2, decreasing the preexisting negative biases, and in some instances introducing a small positive bias, and increasing the preexisting positive biases. As a result, the RMSD was reduced by the assimilation at five of the eleven sites. At SBR and LHS the RMSD was increased by a large amount, and overall the mean RMSD was increased from 16.4 to 19.2 mm.

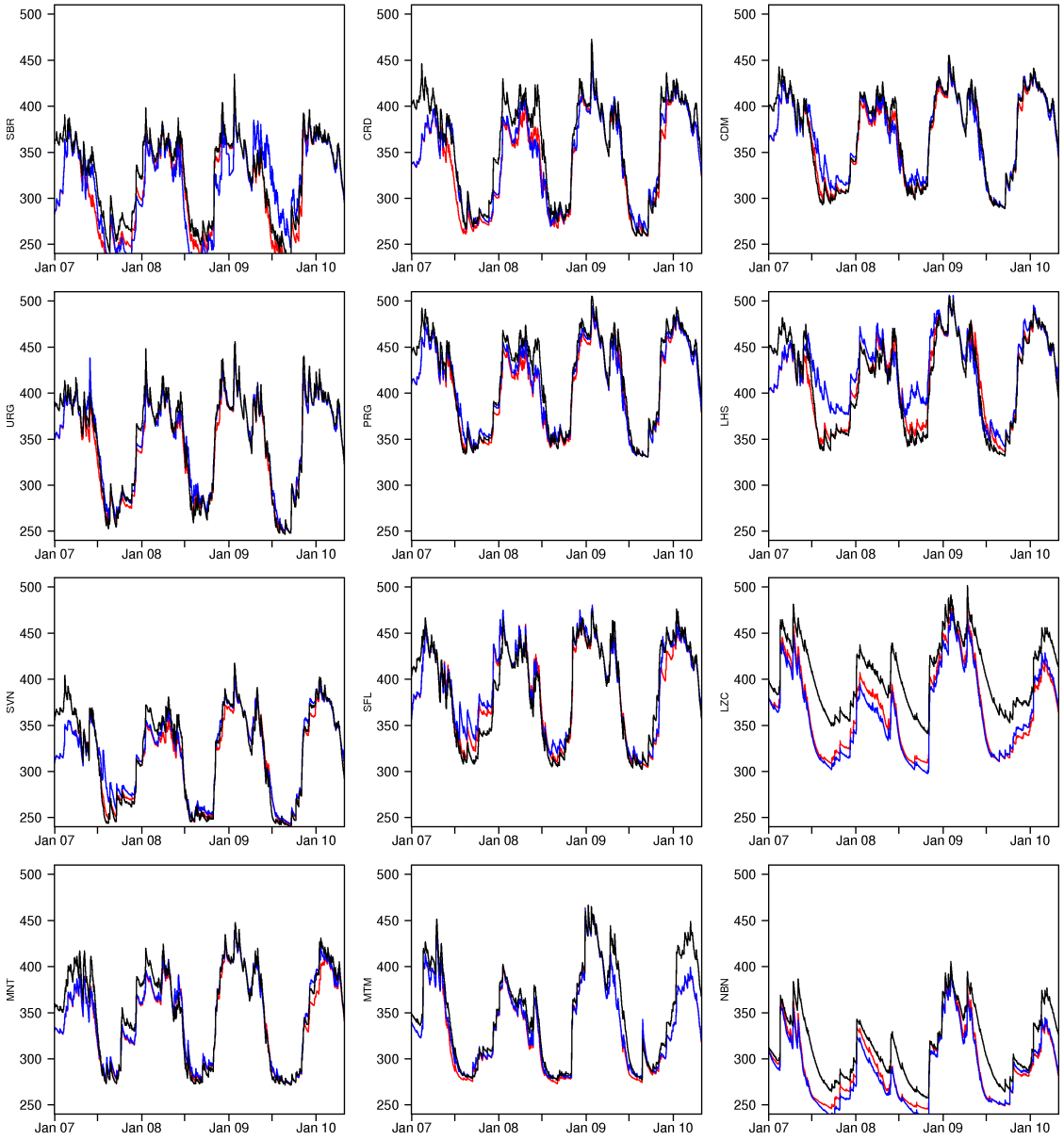

Figure 13. Time series of simulated ω_2 (mm) at each of the SMOSMANIA sites, from SIM_DEL (black), SIM_NRT (red), and SIM_ASCAT (blue).

At many of the SMOSMANIA sites the assimilation degraded the statistics for ω_2, while either having a neutral or slightly positive impact on the ω_1 statistics. This has occurred due to differences in the relative magnitude of the impact of the assimilation on ω_1 and ω_2. For example, at LHS and SFL the small positive bias in ω_2 during each summer was dramatically increased by the assimilation, resulting in the larger bias and RMSD in Table 8. There was also a small positive bias in ω_1 during each summer at these sites, however this was only very slightly increased by the assimilation, so that the net impact of the assimilation on ω_1 was still positive in Table 7 (due to the reduction of negative biases at other times). The results at CDM and SVN were similar, although less extreme: the small positive biases in the SIM_NRT ω_2 during each summer were increased by the assimilation with an overall detrimental impact (although in both instances the negative ω_2 biases in winter were improved). Again the assimilation also enhanced a small positive

bias in ω_1 at these times, however this was insufficient to be detected by the statistics in Table 7. Finally, at LZC and NBN, the larger negative biases and larger RMSD for SIM_ASCAT resulted from reductions in ω_2 late in 2008 and 2009. While the SIM_NRT ω_1 was also negatively biased at these times, the assimilation had very little impact on ω_1, despite the large changes to ω_2.

Table 9 presents the statistics of fit between the SIM_NRT, SIM_ASCAT, and SIM_DEL near-surface soil moisture, and the SMOSMANIA in situ observations. SIM_DEL consistently had better statistics of fit to the SMOSMANIA observations than SIM_NRT, giving substantially higher mean r_{abs} (r_{anm}) for SIM_DEL of 0.70 (0.59), compared to 0.66 (0.53) for SIM_NRT. This suggests that the SMOSMANIA observations are sufficiently accurate to detect the errors associated with the difference

Table 7. Statistics of fit between the SIM_DEL ω_1, and each the SIM_NRT and SIM_ASCT ω_1, from May 2007 to April 2010. For each statistic the best result is indicated in bold, and all correlations are significant at 1%. σ(NRT) indicates the standard deviation of the SIM_NRT time series.

		SIM_NRT/ SIM_DEL				SIM_ASCAT / SIM_DEL			
Site	σ(NRT) (mm)	r_{abs}	r_{anm}	bias (mm)	RMSD (mm)	r_{abs}	r_{anm}	bias (mm)	RMSD (mm)
SBR	0.0055	**0.96**	**0.95**	-0.0012	0.0020	0.95	0.94	**-0.0010**	0.0020
URG	0.0075	0.96	0.94	-0.0017	0.0028	0.96	0.94	**-0.0014**	**0.0025**
CRD	0.0068	0.93	0.91	-0.0017	0.0030	**0.94**	0.91	**-0.0014**	**0.0028**
PRG	0.0086	**0.98**	0.96	-0.0010	0.0021	0.97	0.96	**-0.0007**	0.0021
CDM	0.0085	**0.98**	**0.97**	-0.0007	**0.0019**	0.97	0.96	**-0.0005**	0.0020
LHS	0.0095	**0.96**	0.93	-0.0013	0.0031	0.95	0.93	**-0.0009**	0.0031
SVN	0.0082	0.96	0.94	-0.0018	0.0030	0.96	0.94	**-0.0016**	**0.0029**
MNT	0.0089	**0.96**	0.94	-0.0018	0.0030	0.95	0.94	**-0.0016**	0.0030
SFL	0.0098	0.95	0.92	-0.0011	0.0033	**0.96**	0.92	**-0.0008**	**0.0031**
MTM	0.0074	0.96	0.95	-0.0009	0.0022	**0.97**	0.95	**-0.0008**	0.0022
LZC	0.0077	0.96	0.95	-0.0007	0.0022	**0.97**	0.95	**-0.0006**	**0.0021**
NBN	0.0072	0.97	0.96	-0.0005	0.0017	**0.98**	**0.97**	**-0.0004**	**0.0016**

Table 8. Statistics of fit between the SIM_DEL ω_2, and each the SIM_NRT and SIM_ASCT ω_2, from May 2007 to April 2010. For each statistic the best result is indicated in bold, and all correlations are significant at 1%. σ(NRT) indicates the standard deviation of the SIM_NRT time series.

		SIM_NRT / SIM_DEL				SIM_ASCAT / SIM_DEL			
Site	σ(NRT) (mm)	r_{abs}	r_{anm}	bias (mm)	RMSD (mm)	r_{abs}	r_{anm}	bias (mm)	RMSD (mm)
SBR	47.6	**0.98**	**0.95**	-12.0	**16.0**	0.87	0.86	**-7.7**	24.2
URG	40.5	0.99	**0.96**	-5.1	9.8	0.99	0.95	**0.5**	**9.6**
CRD	42.8	**0.97**	**0.92**	-14.9	19.8	0.96	0.88	**-9.2**	**17.4**
PRG	37.0	**0.99**	**0.98**	-9.7	13.0	0.98	0.97	**-6.0**	**11.6**
CDM	35.6	**0.99**	**0.98**	-3.1	**6.6**	0.97	0.95	**0.9**	12.5
LHS	37.4	**0.98**	**0.93**	**4.0**	**10.4**	0.93	0.85	14.2	24.2
SVN	38.1	**0.99**	**0.96**	**-2.1**	**9.3**	0.98	0.90	2.4	11.4
MNT	38.0	0.98	**0.96**	-4.8	11.9	0.98	0.95	**-2.2**	**10.6**
SFL	37.0	**0.97**	**0.92**	**2.0**	**13.6**	0.96	0.87	6.3	16.2
MTM	45.2	0.97	0.95	-13.5	19.4	0.97	0.95	**-11.1**	**18.2**
LZC	43.8	0.95	0.95	**-38.1**	**40.9**	0.95	0.95	-42.5	45.1
NBN	35.1	0.93	0.94	**-21.9**	**25.9**	0.93	0.94	-26.0	29.2

in forcing used for SIM_NRT and SIM_DEL. Consistent with the results from Table 7, assimilating the ASCAT data slightly improved the statistics at most sites, giving a mean r_{abs} (r_{anm}) of 0.67 (0.54). There is some correspondence between the results relative to the SMOSMANIA observations and relative to SIM_DEL, and at those sites where the greatest improvements relative to SMOSMANIA occurred (URG, CRD, PRG, and MTM) were also improved relative to the SIM_DEL ω_2 in Table 8. Finally, the bias and RMSD relative to SIM_DEL, as well as the fit to the SMOSMANIA observations were improved at MTM by assimilating the ASCAT data, despite it being established in Section 4 that the ASCAT data were of low quality at this site. For the comparison to SIM_DEL, these improvements were due to a small reduction in the negative bias in ω_2 during each summer. The net impact of the assimilation in Figure 13 was much smaller at MTM than at the other sites, since the error covariance for the observations was much higher at this sites (the median was 0.09 m^3m^{-3}, compared to median values typically less than 0.05 m^3m^{-3} at the other sites), and the positive result here was likely due to chance.

Table 9. Statistics of fit between the in situ observations from SMOSMANIA, and the SIM_NRT, SIM_ASCAT, and SIM_DEL ω_1, from May 2007 to April 2010. All statistics are calculated using only days on which all data sets are available, and the RMSD is based on normalised model time series. For each statistic the best result between SIM_NRT and SIM_ASCAT is indicated in bold, and all correlations are significant at 1%.

	SIM_NRT			SIM_ASCAT			SIM_DEL		
Site	r_{abs}	r_{anm}	RMSD (m^3m^{-3})	r_{abs}	r_{anm}	RMSD (m^3m^{-3})	r_{abs}	r_{anm}	RMSD (m^3m^{-3})
SBR	0.77	0.65	0.037	**0.78**	0.65	**0.036**	0.80	0.68	0.036
URG	0.64	0.66	0.111	**0.67**	**0.67**	**0.106**	0.71	0.69	0.100
CRD	0.70	0.56	0.038	**0.73**	**0.57**	**0.036**	0.72	0.57	0.037
PRG	0.68	0.46	0.060	**0.70**	**0.47**	**0.058**	0.71	0.47	0.057
CDM	**0.72**	0.54	**0.057**	0.71	0.54	0.058	0.76	0.55	0.053
LHS	0.65	0.45	0.071	0.65	0.45	0.071	0.71	0.47	0.065
SVN	0.63	0.53	0.085	**0.64**	0.53	**0.084**	0.68	0.52	0.079
MNT	0.55	0.52	0.100	**0.56**	0.52	**0.098**	0.64	0.54	0.090
SFL	0.67	0.45	0.063	0.67	**0.46**	0.063	0.72	0.48	0.058
MTM	0.50	0.41	0.043	**0.55**	**0.46**	**0.041**	0.60	0.47	0.039
LZC	0.71	0.62	0.056	**0.72**	0.62	0.056	0.74	0.62	0.054
NBN	0.67	0.49	**0.057**	0.67	0.49	0.058	0.66	0.48	0.059

6.2.2 Comparison of SIM_NRT and SIM_DEL

The very strong correlations between SIM_DEL and SIM_NRT soil moisture at the SMOSMANIA sites suggest that the temporal information in the DEL and NRT SAFRAN analyses is very similar. Additionally, the development of biases in the SIM_NRT soil moisture suggests the gradual accumulation of systematic errors from the NRT SAFRAN forcing. Figure 14 shows maps of the r_{abs}, r_{anm}, and bias between ω_2 from SIM_NRT and SIM_DEL from May 2007 to April 2010, demonstrating that this behaviour is repeated across France. The correlations between SIM_NRT and SIM_DEL are persistently very high. For r_{abs} 88% of the model grids are above 0.90, and the mean is 0.95, while for r_{anm} 87% of the model grids are above 0.90 and the mean is 0.94. The correlations are slightly lower in mountainous terrain.

Additionally, there is a strong tendency for the SIM_NRT ω_2 to be biased low, and there are only very few isolated locations where the bias is positive, resulting in a mean bias over the plotted period of –13.3 mm. The low bias in the SIM_NRT ω_2 is caused by a substantial low bias in the NRT precipitation forcing. This precipitation bias, plotted in Figure 15, can be very large, and there is a

reasonably strong correspondence between the biases in ω_2 in Figure 14 and in precipitation in Figure 15, including the same isolated areas of positive bias.

These findings have several implications for the following assessment of the SIM_ASCAT assimilation results. First, the agreement between the SIM_DEL and SIM_NRT is already very good, and consequently for the ASCAT soil moisture observations to improve the SIM_NRT simulation will require that those observations be very accurate. Secondly, the principal difference between SIM_DEL and SIM_NRT is a low bias in the NRT soil moisture, and the assessment of the impact of assimilating the ASCAT data is focused on determining whether the assimilation can correct for this bias.

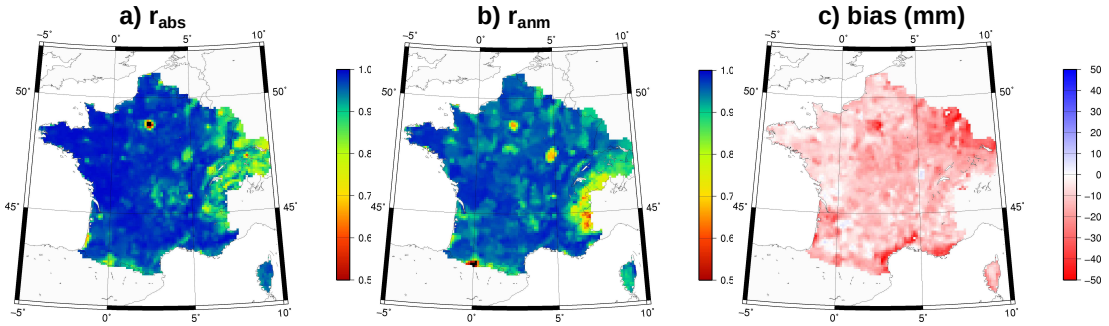

Figure 14. Absolute correlation, anomaly correlation, and bias of SIM_NRT ω_2, relative to SIM_DEL ω_2 (liquid plus solid), from May 2007 to April 2010.

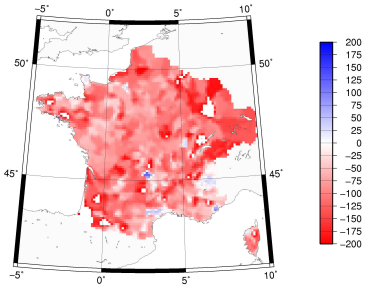

Figure 15. Precipitation bias for SIM_NRT forcing, relative to SIM_DEL, for May 2007 to April 2010 (mm year^{-1}).

6.2.3 Comparison to SIM_DEL soil moisture: temporal averages

Figure 16 shows maps of the mean bias between SIM_DEL and each of SIM_NRT and SIM_ASCAT, for both ω_1 and ω_2. ω_1 also has a negative bias across most of the domain, with a mean of –0.0013 mm (the very small value is associated with the small water reservoir defined by ω_1), and there is only a weak spatial association between the biases in ω_1 and ω_2. The corresponding maps of the RMSD between each experiment and SIM_DEL are shown in Figure 18, demonstrating that in general the RMSD is largest where the bias is largest.

Figure 17 shows the net volume of moisture added by the assimilation of the ASCAT data. Consistent with the negative biases in the soil moisture (relative to SIM_DEL) in Figure 16, moisture is added to the surface across the domain, with a mean of 38.5 mm year^{-1}. There are a handful of isolated locations where net moisture was removed, however these do not correspond to the locations of the positive precipitation and soil moisture biases in Figures 14 and 15. In general, there is no particular correspondence between the maps of the net increments and the maps of the net soil moisture biases, although this could be due to the non-linearity of the relationship between soil moisture increments

and changes in the soil moisture storage, or other complicating factors such as the frequency of the observations.

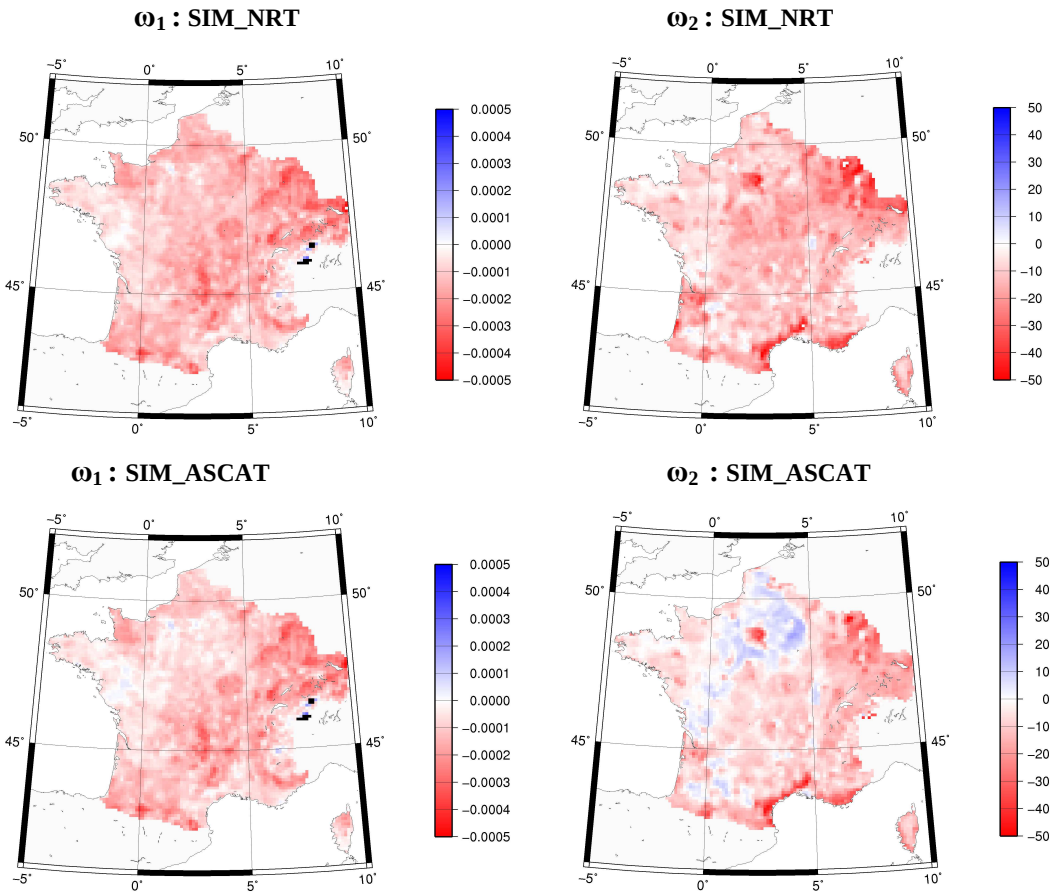

Figure 16. Soil moisture bias (liquid plus solid) relative to SIM_DEL for ω_1 (left) and ω_2 (right), for SIM_NRT (upper) and SIM_ASCAT (lower), from May 2007 to April 2010.

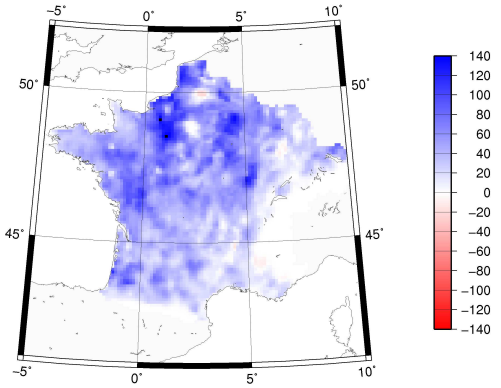

Figure 17. Map of the net analysis increment (mm year^{-1}) added to ω_1 and ω_2 , from May 2007 to April 2010.

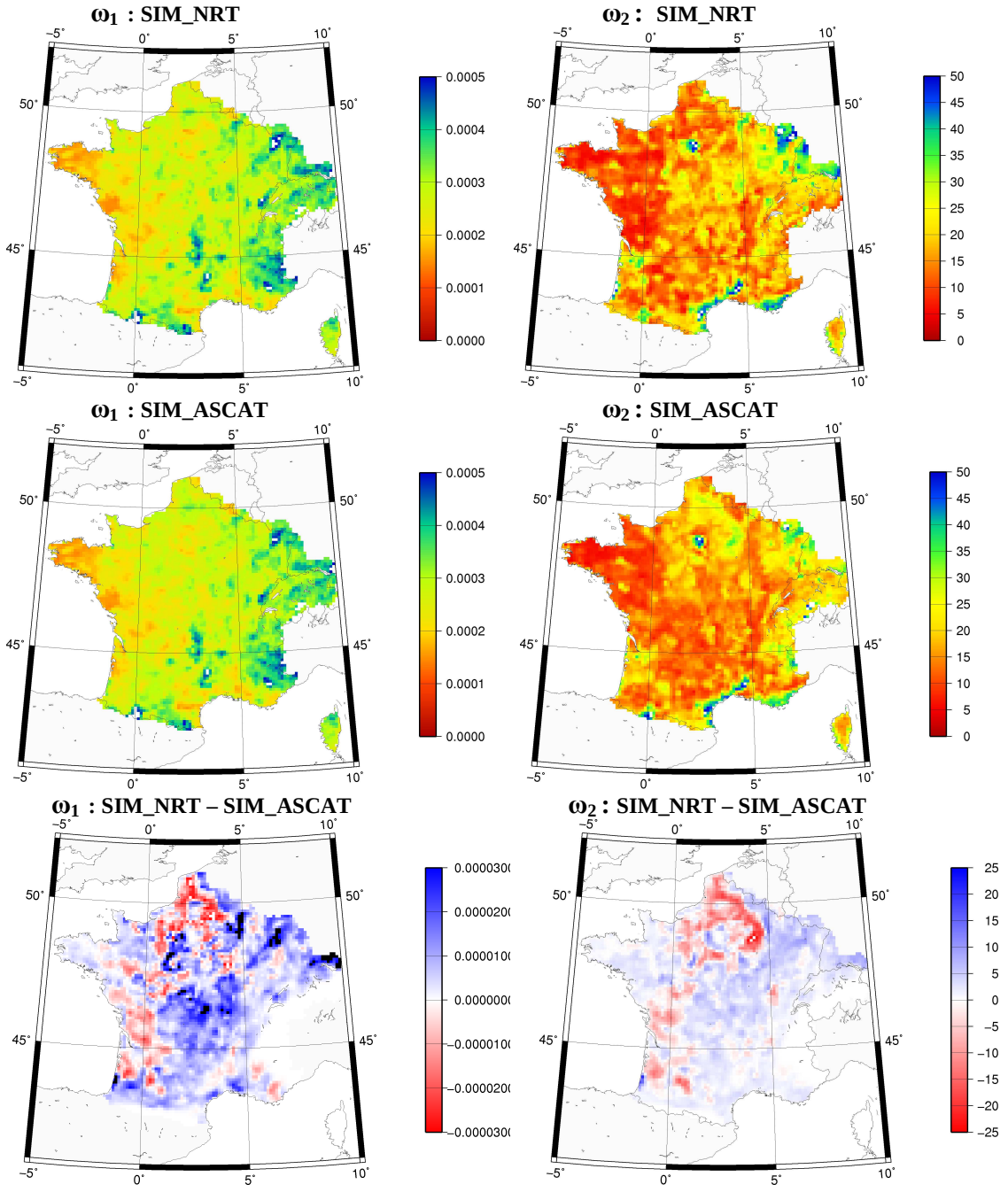

Figure 18. Soil moisture RMSD (liquid plus solid) relative to SIM_DEL for ω_1 (left) and ω_2 (right), for SIM_NRT (upper) and SIM_ASCAT (middle), and the difference between the SIM_NRT and SIM_ASCAT RMSD (lower), from May 2007 – April 2010.

By adding moisture to the surface, the assimilation has reduced the negative biases in ω_1 and ω_2 in Figure 16. For ω_1, the net bias was reduced at most locations (at 78% of the grid cells, and at 94% for which ASCAT observations were available), with the strongest reductions occurring in the north of France, and the mean bias was reduced to –0.0011 mm (from –0.0013 mm). For ω_2 the negative biases were also reduced across most of France, however there is now a region in the northeast with a

small positive bias (corresponding to very small negative biases in ω_1 for SIM_NRT). Examining individual time series for these locations indicates that this positive bias accumulates consistently through the assimilation experiment, with the largest increases occurring each spring. Much of this region of increased bias has an unusual soil type (the Champagne-Picardie region), with dark soils and a large soil moisture holding capacity, which are not well represented by soil parameters used in SIM. This region also stood out in the original (pre-CDF-matched) ASCAT data in Figure 9, as having ASCAT observations higher than the SIM ω_1. Overall, the assimilation reduced the mean bias for ω_2 to –7.9 mm (form –13.3 mm), while the absolute bias was reduced at 73% of the grid cells (and at 89% of the grids for which ASCAT data were available).

Figure 18 shows that for both ω_1 and ω_2, the assimilation decreased the RMSD across most of France, although it is increased it in the northeast and southwest, corresponding to those locations where the small positive bias was introduced in to ω_2. For ω_1, the assimilation reduces the RMSD at 59% of the grid cells (and at 71 % of cells for which ASCAT data were available), giving a slight reduction in the mean RMSD from 0.00283 mm for SIM_NRT to 0.00279 mm for SIM_ASCAT. For ω_2, the RMSD was reduced for 57% of the grid cells (and at 69 % of cells for which ASCAT data were available), although there were relatively large increases in the RMSD in the northeast. Overall, the mean RMSD was reduced from 18.1 to 17.6 mm.

6.2.4 Comparison to SIM_DEL soil moisture: spatial averages

Figure 19 shows the temporal evolution of the mean soil moisture from each of the experiments, while Figure 20 shows the temporal evolution of the difference between each of SIM_NRT and SIM_ASCAT, and the SIM_DEL soil moisture. The ω_1 time series is very noisy, making it difficult to distinguish between the three experiments in Figure 19. However, Figure 20 shows that there was a consistent low bias in the SIM_NRT ω_1. In contrast, for ω_2 there is a greater distinction between the three time series. SIM_NRT was persistently biased low, and in both 2007 and 2009 the bias increased substantially (to around 20 mm) towards the end of summer. There was a low bias in the SIM_NRT ω_2 at the start of the experiments in January 2007, associated with a substantial low bias in SIM_NRT in the southwest of France at that time. However, this low bias did not persist for long, and was lost within the first few months (by April 2008 the bias in ω_2 in Figure 20 was quite small).

Figure 21 shows the timseries of the average volume of moisture added by SIM_ASCAT each day. Very little moisture was added or subtracted during the winter months, due largely to the widespread occurrence of frozen surface conditions. During the nonwinter months there was a tendency towards the net addition of moisture to the surface (although there were periods of net moisture removal). For ω_1 this resulted in a slight reduction in the negative biases, although the assimilation had little impact on the RMSD. For ω_2 the reduction in the biases generally increased through the summer, and persists into early winter, before being lost by the end of winter. For most of the time period this resulted in a substantial reduction in the RMSD between the simulated ω_2 and SIM_DEL.

There were two exceptions to the positive impact of the assimilation on the RMSD. The first occurred in June 2009, when the assimilation enhanced preexisting negative biases in the north of France and near Les Landes in the southwest. The second occurred in September 2009, and was due to a particularly large bias in SIM_ASCAT data (relative to SIM_DEL) in the Champagne-Picardie region at that time.

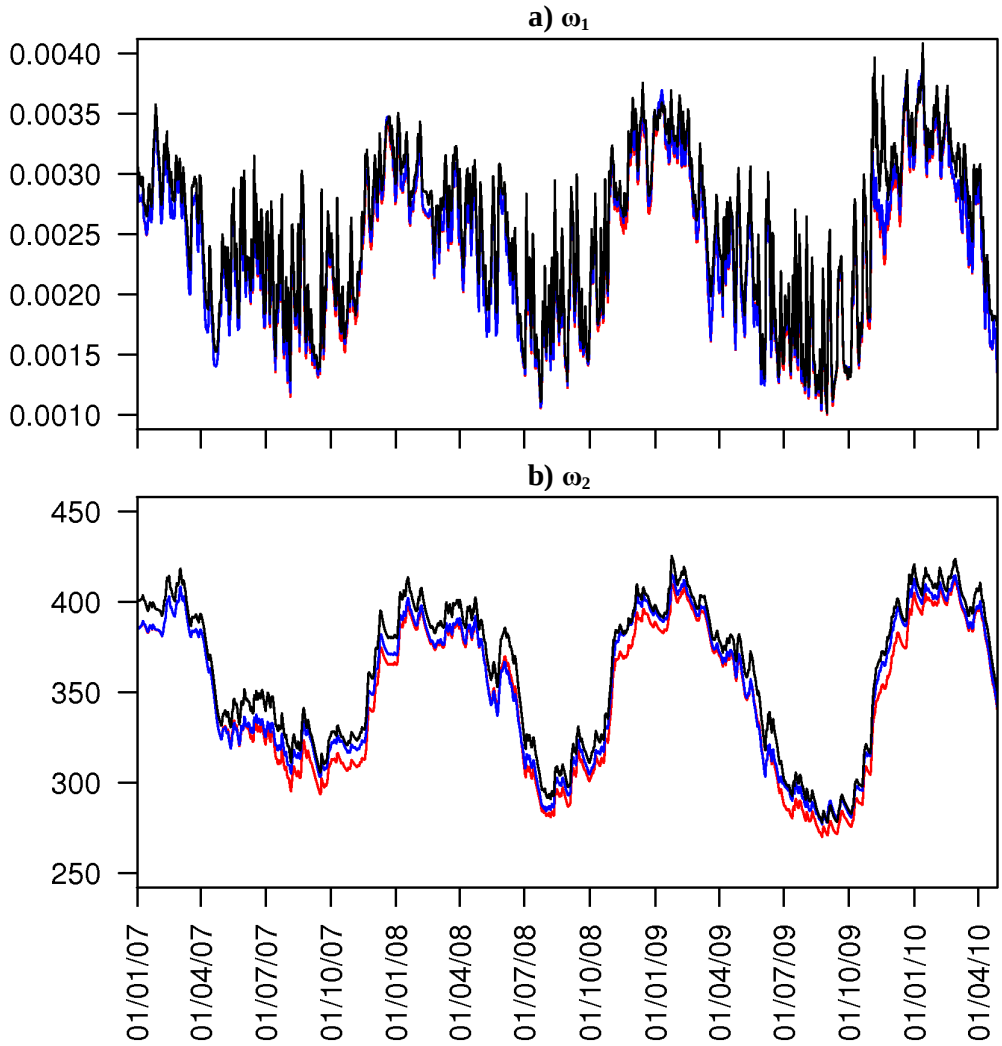

Figure 19. Time series of the spatial mean a) ω_1 and b) ω_2 , in mm for SIM_DEL (black), SIM_NRT (red) and SIM_ASCAT (blue).

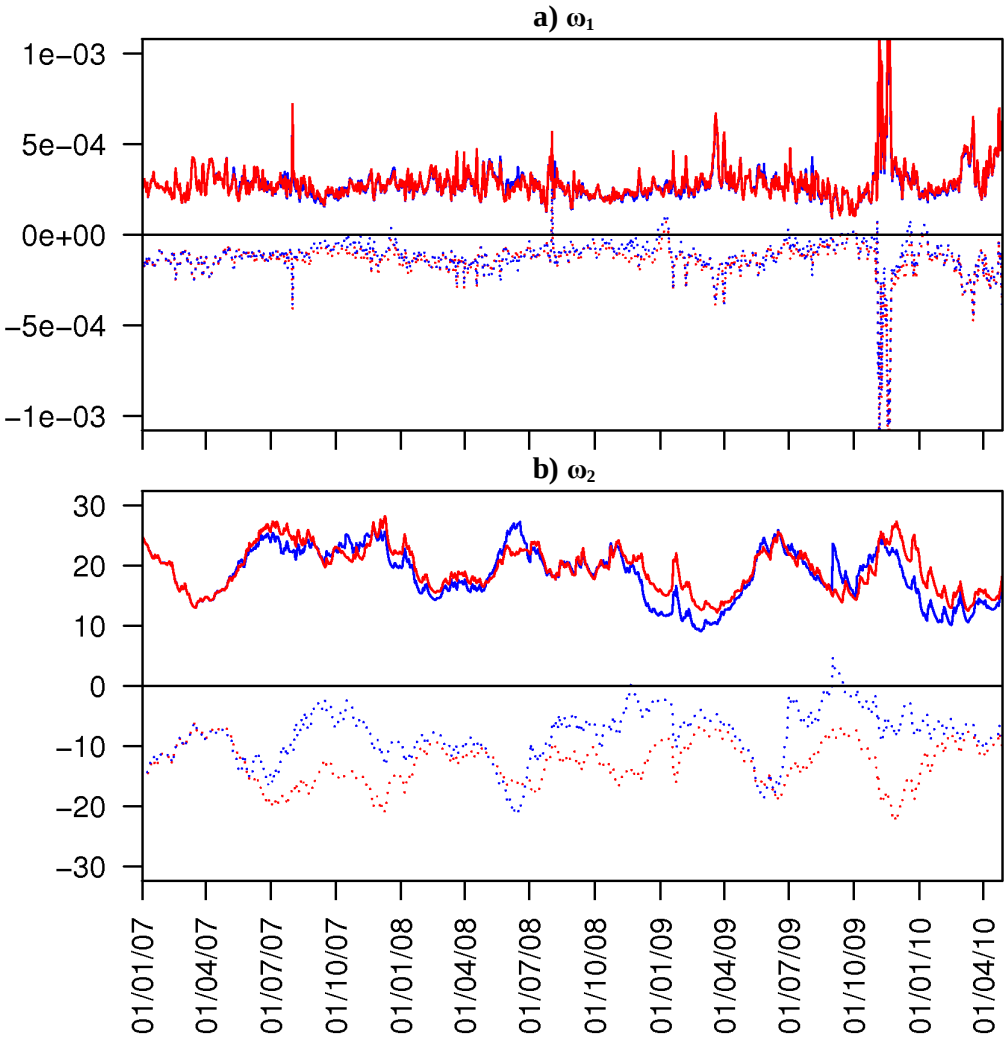

Figure 20. Time series of the spatial mean bias (dotted lines) and RMSD (solid lines) in mm, for a) ω_1 and b) ω_2 relative to SIM_DEL for SIM_NRT (red) and SIM_ASCAT (blue).

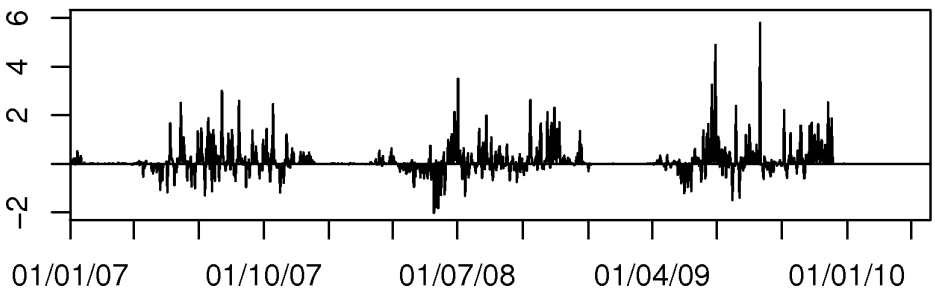

Figure 21. Time series of the spatial mean volume of moisture (mm day^{-1}) added to the surface moisture (to ω_1 and ω_2) through assimilation of the ASCAT SDS.

6.2.5 Impact on the surface water balance

Figure 22 shows the time series of the monthly mean of each of the surface water balance terms, averaged across France, for each of SIM_DEL, SIM_NRT, and SIM_ASCAT, while Figure 23 shows the time series of the mean monthly bias (relative to SIM_DEL) of each term for SIM_NRT and SIM_ASCAT. Precipitation is imposed by the forcing, while all other variables are output from ISBA. The precipitation in SIM_NRT (and SIM_ASCAT) was persistently biased low (the only positive monthly bias was 1.5 mm month^{-1} in April 2007), with a tendency for larger biases in winter, generating a large mean monthly bias of -16.8 mm month^{-1}.

Also included in the plot is the mean monthly volume of moisture added to the soil column by the SEKF in the SIM_ASCAT experiment. The largest monthly increments were of the order of 10 mm month^{-1}, which is similar in magnitude to the precipitation errors. The increments were lower during the winter months (as they were in the daily plot in Figure 21), giving a mean increment of +2.9 mm month^{-1}.

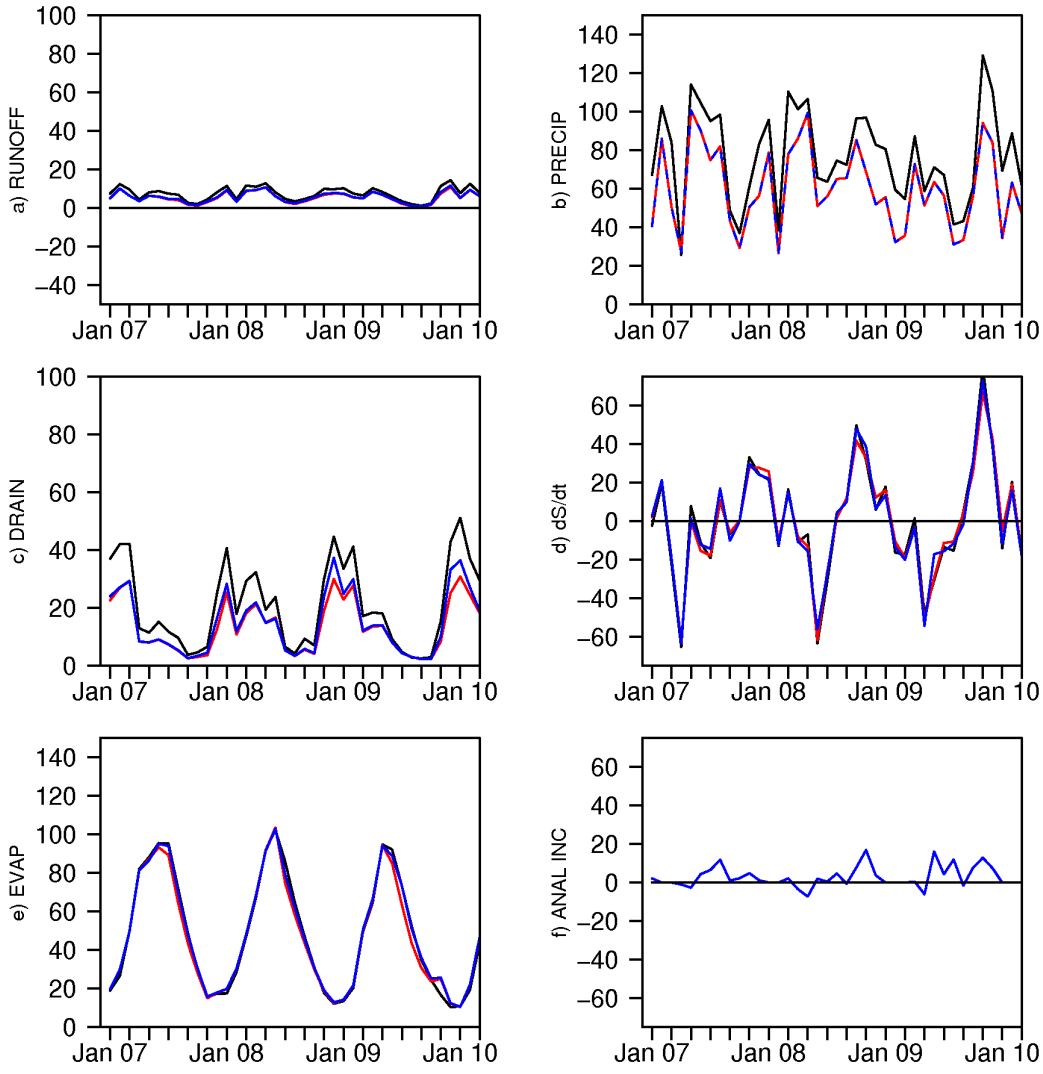

Figure 22. Monthly water balance in mm month^{-1} for SIM_DEL (black), SIM_NRT (red), and SIM_ASCAT (blue). Each panel shows a) runoff, b) precipitation, c) drainage, d) change in surface moisture storage (including ω_2 and ω_3, liquid and solid), e) evapotranspiration, and f) the analysis increments (for SIM_ASCAT).

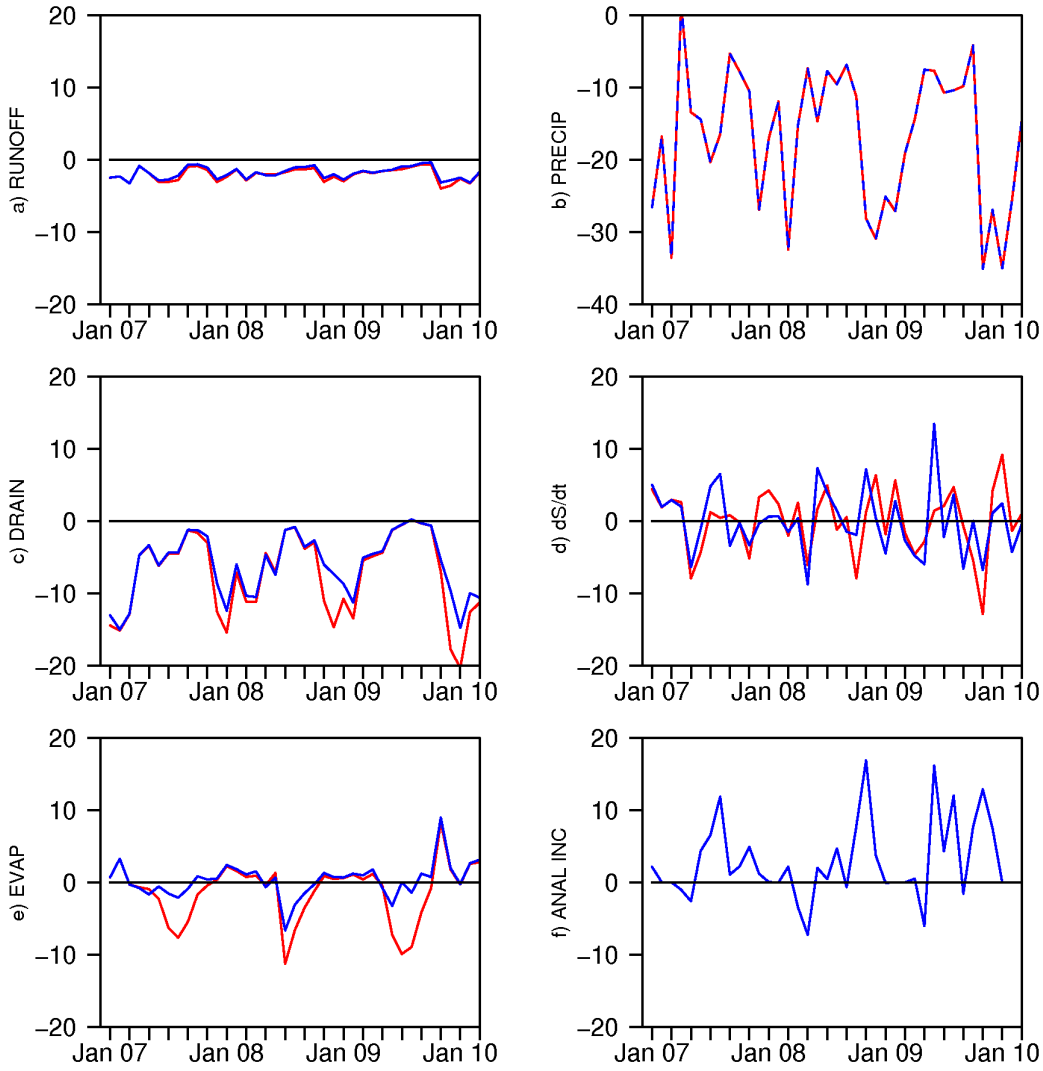

Figure 23. Error relative to SIM_DEL of the monthly water balance terms for SIM_NRT (red) and SIM_ASCAT (blue). Each panel shows a) runoff, b) precipitation, c) drainage, d) change in surface moisture storage (including ω_2 and ω_3, liquid and solid), and e) evapotranspiration, together with f) the analysis increments (for SIM_ASCAT).

Close to half of the precipitation bias between SIM_NRT and SIM_DEL is transferred into a bias in the drainage term. The SIM_NRT drainage was persistently biased low (the only positive monthly bias was 0.2 mm month^{-1} in August 2009), with the largest biases occurring in winter, when the largest drainage was generated. Over the entire period the mean monthly bias was -7.3 mm month^{-1}. Runoff has a similar seasonal cycle to drainage (both are triggered once the model soil moisture exceeds saturation), although it is much smaller. The runoff was also biased low every month, with larger biases in winter when more runoff was generated, giving a mean monthly bias of -2.0 mm month^{-1}. For both discharge and runoff the bias was close to 30% of the SIM_DEL forecasts (compared to a precipitation bias of 20%). In both cases, the addition of moisture to the surface (mostly during the nonwinter months) in SIM_ASCAT reduced the negative biases, to –6 mm month^{-1} and -1.8 mm month^{-1}, respectively (equivalent to 17% and 10% of the SIM_NRT bias). The increased drainage (and to a lesser extent runoff) for SIM_ASCAT explains why the reduction in the negative ω_2 bias for SIM_ASCAT was gradually lost throughout winter in Figures 19 and 20.

Evapotranspiration has the opposite seasonal cycle to drainage and runoff, with the greatest fluxes in summer. In each year the SIM_NRT evapotranspiration forecasts were biased low in late-summer, during the decreasing phase of the annual peak, when the drier surface conditions cause transpiration to be limited by moisture availability. These low evaporation biases (of greater than -5 mm month^{-1}) were then balanced by small positive values during the wet months (approximately 1 mm month^{-1}), generating a mean bias of -1.2 mm month^{-1}. This bias was just 2% of the SIM_DEL forecast precipitation, and is very small given that evaporation is one of the largest terms in the water balance (together with precipitation). Assimilating the ASCAT data effectively decreased the transpiration bias during summer, while having very little impact on the positive bias during winter (which will not have been related to soil moisture), generating an overall reduction of the bias to +0.4 mm day^{-1} (or 70% of the original bias, with a reversal of sign).

The change in the surface moisture storage was the least consistent of the surface water balance terms. The seasonal cycle in the soil moisture storage (which includes liquid and frozen ω_2 and ω_3) is similar to that in ω_2 in Figure 19, and consists of a dry summer mode and a wet winter mode. The transition between these modes tends to be abrupt, so that in each year there was one month early in the summer (winter) in which there was a large negative (positive) change in the soil moisture storage. There is no clear pattern in the SIM_NRT biases in the monthly change in moisture storage, except perhaps a slight tendency to underestimate the changes in soil moisture - for both positive and negative changes. The mean bias in the change in storage is rather small, at just 0.1 mm month^{-1} The impact on the assimilation on the change in moisture storage is less consistent than for the surface moisture fluxes, and there were instances of the assimilation generating both increased and decreased monthly errors. Overall the mean bias is unchanged from 0.1 mm month^{-1}, likely since it was already very small.

6.2.6 Impact on the MODCOU river discharge

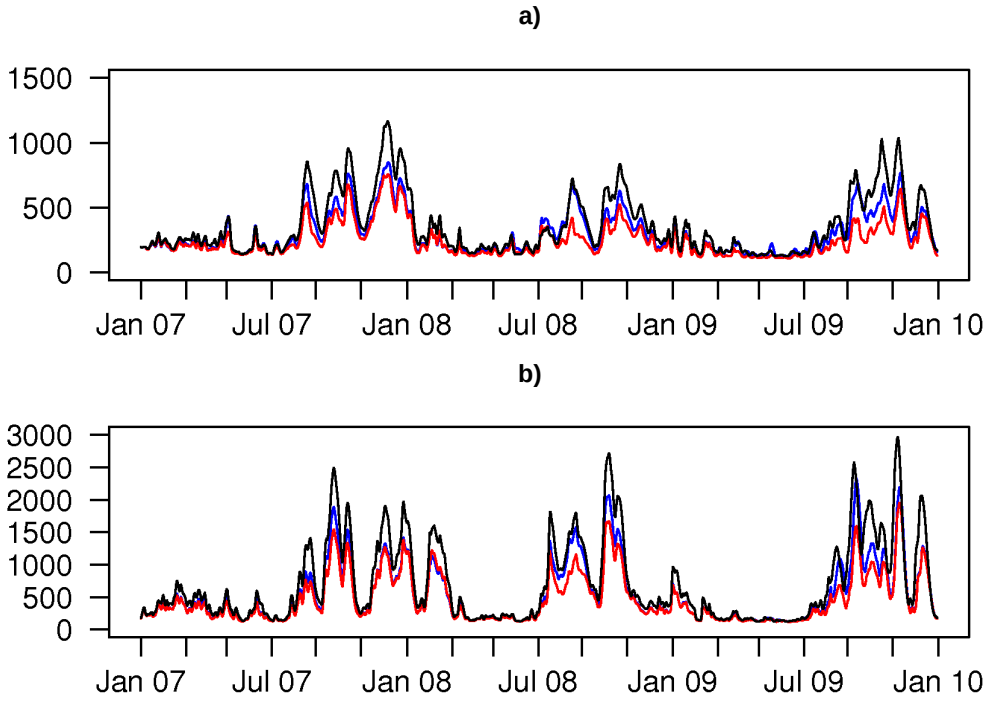

Figure 24. Simulated discharge (m^3 day^{-1}) for the a) River Seine at Poses and b) the Loire River at Montjean sur Loire, from SIM_DEL (black), SIM_NRT (red), and SIM_ASCAT (blue).

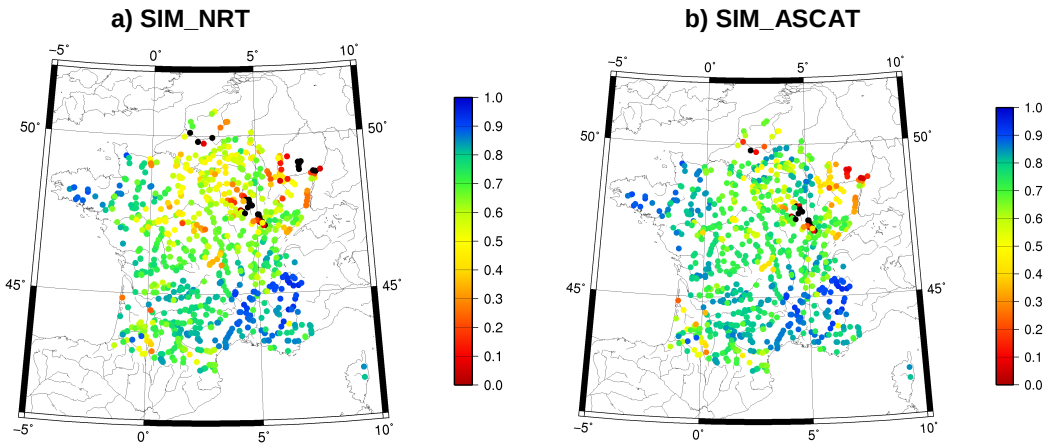

Figure 25. The Nash-Sutcliffe efficiency simulated at each gauging station, assuming SIM_DEL as the truth, for a) SIM_NRT (left) and b) SIM_ASCAT.

The fluxes generated by SIM for each experiment have been routed through the surface river network using the MODCOU model. Figure 24 shows two examples of the resulting daily simulated river flows, for the Seine and Loire rivers, at locations close to each river outlet. Consistent with the previous results for soil moisture, the temporal variability in the SIM_NRT simulated river discharge agreed very well with the SIM_DEL simulations, while the net flow was biased low. Additionally, the impact of the assimilation was largely limited to increasing the magnitude of the peak flows. In most instances, the assimilation increased the peak flows to be closer to the SIM_DEL time series, while having little impact on the timing of the peak flows. For example the assimilation has not corrected the slight delay in the timing on the peak flows around September 2009 for the Loire river.

Figure 25 shows a map of the Nash-Sutcliffe Efficiency (E) at each of the 907 gauging stations modeled by MODCOU. Most (68%) of the stations have E greater than 0.6, although the efficiency is in general lower (between 0.4 and 0.6) in the northwest. The mean across all of the stations is 0.62. There are 23 stations with negative values, all of which have very small upstream catchment areas, resulting in very low discharge (maximum value ~100 m^3 day^{-1}) and an increased sensitivity to errors in the precipitation forecasts. Figure 25 also includes a map of E for the SIM_ASCAT experiment, while Figure 26 compares the E for each experiment. The assimilation increased E at most (82%) locations, with the greatest increases occurring in the northwest, where the SIM_NRT E was lower. For SIM_ASCAT, 81% of the gauging stations had an efficiency above 0.6, and overall, the mean efficiency was increased to 0.68. Ten of the stations that had negative E for SIM_NRT have positive values for SIM_ASCAT, however plots comparing the improvement in the statistics against the size of the upstream catchment (not shown) did not show a relationship between the two.

Figure 27 shows the discharge ratio (Q_{SIM_NRT}/Q_{SIM_DEL}) at the same gauging stations plotted in Figure 24. For SIM_DEL, the ratio was between 0.5 and 0.8 at most stations, with a mean of 0.68. Since the assimilation added moisture across France the discharge ratio was increased, particularly in the north. At 31 locations (nearly all in the north), the assimilation generated discharge ratios above one, however the scatterplot in Figure 28 shows that at most of these locations the SIM_ASCAT ratio was still closer to one than SIM_NRT was. Overall, the absolute error in the discharge ratio was decreased at 88% of the gauging stations, and the mean ratio was increased to 0.76.

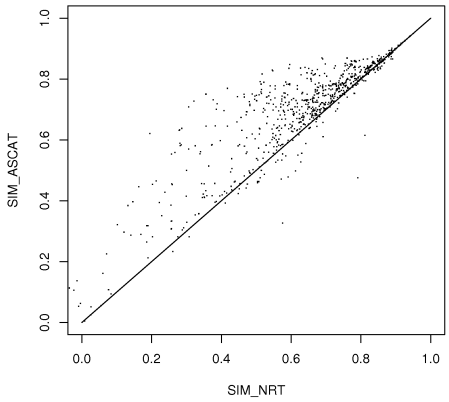

Figure 26. Scatterplot of the Nash-Sutcliffe efficiency, assuming SIM_DEL as the truth, for SIM_ASCAT vs. SIM_NRT.

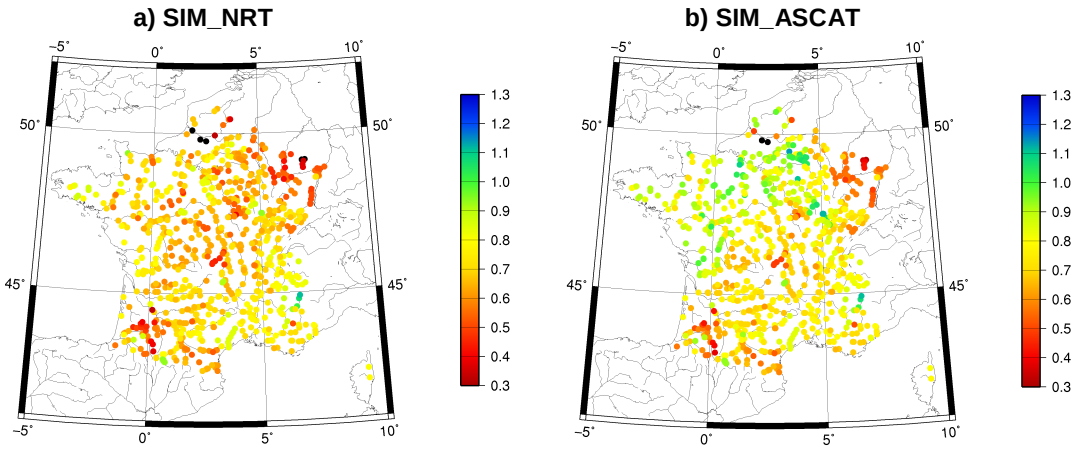

Figure 27. The discharge ratio simulated at each gauging station, assuming SIM_DEL as the truth, for a) SIM_NRT and b) SIM_ASCAT.

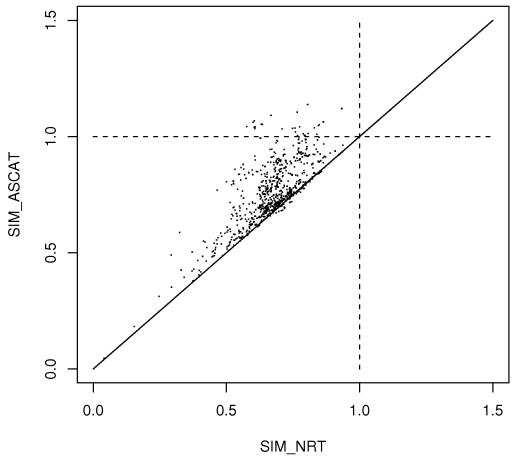

Figure 28. Scatterplot of discharge ratio, assuming SIM_DEL as the truth, for SIM_ASCAT vs. SIM_NRT.

7 Summary and conclusions

This report presents an assessment over France of the 12.5 km ASCAT surface degree of saturation soil moisture product disseminated by EUMETSAT. The ASCAT SDS observations have been assessed from January 2007 to April 2010 by comparison to in situ soil moisture observations from the SMOSMANIA network, by comparison to near-surface soil moisture from the SIM hydrological model, and by testing the impact of assimilating the ASCAT data into the SIM model. Each of these comparisons indicated that the ASCAT SDS can accurately detect changes in near-surface soil moisture.

Before being assessed, the ASCAT data were quality controlled to remove observations potentially contaminated by open water, vegetation, complex topography, urban regions, and frozen surface cover. Initial plots of the ASCAT SDS indicated that the frozen surface flag calculated during the retrieval of the SDS from ASCAT backscatter observations does not accurately detect all instances of frozen surface conditions. Consequently, frozen conditions resulted in anomalously low SDS values. As pointed out by Pellarin et al. (2006) these values are problematic when an exponential filter (or assimilation into a more complex soil profile model) is used to extrapolate the SDS to a deeper-layer soil moisture, due to the long memory of the anomalously low values in the filtered time series. The ASCAT SDS should then be screened to remove observations of frozen surface conditions based on ancillary data, before an exponential filter or data assimilation is applied. In this report, a frozen surface mask has been applied to the ASCAT data, based on SIM simulations of nonzero frozen soil moisture in the near-surface layer.

The ASCAT SDS data had a strong temporal relationship with the in situ observations of near-surface soil moisture from the 12 monitoring stations in the SMOSMANIA network in southwest France. The one exception is at the MTM site, which is located in reasonably steep terrain in the foothills of the Pyrenees. At the remaining sites, the ASCAT SDS consistently had a good qualitative fit to the SMOSMANIA observations, detecting both the main dynamics of the seasonal cycle, as well as the short-term response to rain events. Consequently, the correlation and anomaly correlation between the two data sets were significant at all SMOSMANIA sites, and consistently high, with mean values of 0.70 and 0.62, respectively.

Soil moisture from the SIM hydrological model has also been compared to the observations at the SMOSMANIA sites. At the seasonal scale, the temporal agreement between the near-surface soil moisture from SIM and SMOSMANIA was similar to that between ASCAT and SMOSMANIA, and the absolute correlations did not favour either ASCAT or SIM. The anomaly correlations were generally better for ASCAT, suggesting that it can better predict short-term variability in the SMOSMANIA time series. However, the temporal association between the ASCAT and SIM time series was consistently better than the association between either of these data sets and SMOSMANIA. Visually, ASCAT and SIM have a similar degree of short-term variability, and the correlations and anomaly correlations between ASCAT and SIM were consistently higher than those for SMOSMANIA, with a mean correlation of 0.75 and a mean anomaly correlation of 0.70. This result is consistent with the greater similarity between the definition of the soil moisture estimated by SIM and ASCAT (both are area-averages over tens of kilometers, with a depth of approximately 1 cm), compared to the SMOSMANIA observations (point-based observations at a depth of 5 cm).

The root mean square of the random error between each SDS data set and the ‘true’ near-surface soil moisture obtained by triangulating these three data sets has been estimated at each of the SMOSMANIA sites, using an additive error model, with a random error component and a constant bias (to account for systematic differences between the data sets). The errors obtained for ASCAT and SIM are lower than those for SMOSMANIA, likely because the truth defined by the three data sets is more strongly influenced by the common definition of ASCAT and SIM. If the resultant root mean

square of the random errors are converted into volumetric errors based on the range of the SMOSMANIA soil moisture at each site, the mean root mean square error across the SMOSMAINA sites was 0.036 m^3m^{-3} for ASCAT, 0.039 m^3m^{-3} for SIM, and 0.047 m^3m^{-3} for SMOSMANIA. The slightly lower estimated error for ASCAT than for SIM suggests that assimilating the ASCAT data into SIM should improve the SIM near-surface soil moisture.

All of the comparisons above were based on the descending pass ASCAT SDS only, following previous findings that soil moisture derived from the ascending ASCAT overpass is less accurate. While comparison of the ascending overpass ASCAT SDS to the SDS time series from SMOSMANIA and SIM confirmed the reduced accuracy of the ascending overpass ASCAT data, the performance of the ascending pass ASCAT data was still quite good, and mean (excluding MTM) correlation and anomaly correlation were 0.71 and 0.62 respectively for the SMOSMANIA time series, and 0.65 and 0.56, respectively for the SIM time series (all correlations were significant). Based on these findings, it is recommended that the SDS data from the descending ASCAT overpass be used in preference to the ascending observations (as has been done for the assimilation experiments presented here). However for applications where more frequent data are required the ascending overpass ASCAT data are sufficiently accurate that they may still be useful.

Additionally, the impact of updating the change-detection model parameters for retrieving the SDS from ASCAT backscatter observations to use model parameters calculated from ASCAT observations, rather than older ERS-derived parameters has also been examined. The results indicated that the updated ASCAT(ASCAT) retrieval method provides a clear improvement over the older ASCAT(ERS) method, with improvements in the dynamic range, short-term variability, and spatial coverage (associated with the increased resolution) of the retrieved observations.

The strong temporal association between the SIM and ASCAT near-surface soil moisture that was observed at the SMOSMANIA sites occurs consistently across France. The correlation and anomaly correlations between SIM and ASCAT near-surface soil moisture were significant at nearly all of the SIM model grids, and the correlations were consistently high, with mean values of 0.68 and 0.61, respectively. Since the SIM and ASCAT soil moisture are derived using totally independent methods, the high level of agreement between them is very strong evidence that both detect accurate near-surface soil moisture dynamics. This strong agreement also supports the assimilation of ASCAT into SIM, since it indicates that both soil moisture estimates are detecting similar physical processes.

Finally, the ASCAT soil moisture data were assimilated into the SIM model over France, from January 2007 to April 2010. The assimilation was performed with a Simplified EKF, since preliminary tests with more sophisticated techniques (an EKF and an Extended Kalman Smoother) did not yield better results, and the positive results obtained here indicate that the SEKF is sufficient. The impact of the assimilation on the model skill was assessed principally by testing whether the assimilation improved the simulations relative to an experiment in which SIM was forced with higher quality forcing (SIM_DEL). The forcing used in the assimilation experiments (SIM_NRT) was already very accurate, making this an ambitious bench-mark for assessing the ASCAT observations, and any improvements obtained here would likely be much greater for a land-surface model forced with lesser quality forcing, for example from an NWP model. Additionally, the temporal variability in the soil moisture from SIM_DEL and SIM_NRT was very similar, and the greatest differences between the two were due to the gradual accumulation of forcing errors in the SIM_NRT soil moisture. Most notably, there was a significant negative bias in the SIM_NRT precipitation forcing of -16.8 mm $month^{-1}$, which resulted in a substantial negative bias in the soil moisture. Consequently, the impact of the assimilation has principally been tested by examining whether it corrected this soil moisture bias.

In this respect assimilating the ASCAT data was very successful, and the assimilation reduced the bias in the simulated root-zone soil moisture at 89% of grids for which ASCAT data was available, reducing the mean bias over the domain from -13.3 to -7.9 mm (over the last three years of the experiment). This led in turn to reductions in the negative bias in run-off (from -2.0 to -1.8 mm month-

^{1}), drainage (from -7.3 to -6.0 mm month^{-1}), and evapotranspiration (from -1.2 to 0.4 mm month^{-1}). The assimilation also reduced the negative bias in the river flow simulations, increasing the mean discharge ratio at 907 stations across France from 0.68 to 0.76 , while also increasing the Nash-Sutcliffe efficiency from 0.62 to 0.68.

While the impact of the assimilation on the model statistics was in general positive, there is some evidence that assimilating the ASCAT SDS had too strong a tendency to add moisture to the model surface, and that the ASCAT observations may not have consistently responded to the same errors that were indicated by the differences between SIM_NRT and SIM_DEL. In particular, the assimilation did not detect the small number of locations where the soil moisture bias was positive relative to SIM_DEL, and there were several examples at the SMOSMANIA sites where the assimilation did not respond to the presence of positive biases in SIM_NRT. Additionally, the fact that the assimilation improved the model statistics (relative to both the SMOSMANIA observations and SIM_DEL) at MTM, despite the poor quality of the ASCAT data there, highlights that it is possible for the assimilation to improve the model ω_2 by improving the biases, even if ASCAT has little skill. It is possible that in these experiments assimilating the ASCAT data had a tendency to add moisture for some other reason (perhaps associated with the CDF-matching technique), and that it was simply chance that this addressed the negative biases relative to SIM_DEL.

The limited impact of the assimilation on the model ω_1 also highlights a weakness in the SIM model for use in near-surface soil moisture assimilation. The assimilation is based on the assumption that errors in ω_1 are largely due to errors in ω_2, and ω_2 is then corrected on this basis. However, in ISBA ω_1 has a limited memory, and the errors in ω_1 (detected by ASCAT) are as likely caused by errors in the model forcing as by preexisting errors in the model soil moisture (in any layer). Despite this, the assimilation is still successful, since the errors generated in ω_1 and ω_2 from incorrect forcing are usually strongly correlated. However, the assimilation can easily over-correct ω_2, and it is also susceptible to the accumulation of large updates to ω_2, when the assimilated observations are biased, since there is often little feedback from ω_2 in the ω_1 forecasts to prevent this.

Despite these uncertainties, the balance of evidence suggests that assimilating the ASCAT SDS had a greater tendency to improve, rather than degrade, the model ω_2 relative to SIM_DEL, since it has improved the absolute fit (as measured by the RMSD) between SIM_NRT and SIM_DEL at 69 % of the model grids for which the ASCAT data were available. This suggests that more often that not ASCAT can accurately detect the errors in SIM_NRT associated with errors in the NRT forcing. Combined with the previously discussed comparisons to the SMOSMANIA observations and SIM near-surface soil moisture these results provide strong support for the accuracy of the ASCAT SDS data.

Finally, the results of this work highlight that hydrological models can be useful tools for assessing novel remotely sensed soil moisture. Models can provide an indication of the accuracy of the remotely sensed data at the continental scale, which is not possible with in situ observations. Additionally, assimilating the soil moisture data into models allows the data to be assessed through examining its impact on other variables, including variables for which observations are available at the continental scale. In this experiment, the bias in the precipitation was amplified in the simulated drainage and runoff forecasts (relative to the net flux for each variable), making the river discharge an ideal variable with which to test whether the assimilation can correct for precipitation errors. It is recommended that this work be extended to also assess the impact of assimilating the ASCAT SDS against observations of river discharge.

8 Acknowledgements

The authors would like to acknowledge Julia Figa-Saldaña from EUMETSAT, and the Institute for Photogrammetry and Remote Sensing at TU-Wien for providing the ASCAT observations presented here. Additionally, we are grateful to Wolfgang Wagner, Stefan Hasenauer, and Vahid Naeimi from TU-Wien for advice regarding the ASCAT data.

9 References

Albergel, C., and co-authors (2008), From near-surface to root-zone soil moisture using an exponential filter: an assessment of the method based on in-situ observations and model simulations, *Hydrology and Earth System Sciences*, 12, 1323–1337.

Albergel, C., C. Rüdiger, D. Carrer, J.-C. Calvet, N. Fritz, V. Naeimi, Z. Bartalis, and S. Hasenauer (2009), ASCAT surface soil moisture products with in-situ observations in southwestern France, *Hydrology and Earth System Sciences*, 13, 115–124.

Albergel, C., and co-authors (2010), Cross evaluation of modelled and remotely sensed surface soil moisture with in situ data in southwestern France, *Hydrology and Earth System Sciences*,14, 2177-2191.

Anguela, P., M. Zribi1, S. Hasenauer, F. Habets, and C. Loumagne (2008). Analysis of surface and root-zone soil moisture dynamics with ERS scatterometer and the hydrometeorological model SAFRAN-ISBA-MODCOU at Grand Morin watershed (France), *Hydrology and Earth System Science*, 12, 1415–1424.

Bartalis, Z., W. Wagner, V. Naeimi, S. Hasenauer, K. Scipal, H. Bonekamp, J. Figa, and C. Anderson (2007), Initial soil moisture retrievals from the METOP-A Advanced Scatterometer (ASCAT), *Geophysical Research Letters.*, 34, L20,401, doi:10.1029/2007GL031088.

Boone, A. J.-C. Calvet, and J. Noilhan (1999), Inclusion of a third soil layer in a land surface scheme using the force-restore method, *Journal of Applied Meteorology*, 38, 1611-1630.

Brocca L., S. Hasenauer, P. De Rosnay, F. Melone., T. Moramarco, P. Matgen , and J. Martínez-Fernández (2010a), *Consistent validation of H-SAF soil moisture satellite and model products against ground measurements for selected sites in Europe*, Associated Scientist Activity in the framework of the Satellite Application Facility on Support to Operational Hydrology and Water Management (H-SAF) Intermediate Report, EUMETSAT H-SAF, pp. 39.

Brocca, L., F. Melone, T. Moramarco, W. Wagner, and S. Hasenauer (2010b), ASCAT soil wetness index validations through in situ modeled soil-moisture data in central Italy, *Remote Sensing of Environment*, inpress. doi:10.1016/j.rse.2010.06.009.

Calvet, J.-C., Fritz, N., Froissard, F., Suquia, D., Petitpa, A., and Piguet, B. (2007): In situ soil moisture observations for the CAL/VAL of SMOS: the SMOSMANIA network, *2007 International Geoscience and Remote Sensing Symposium, Spain*, 23-28 July 2007, 1196-1199.

Calvet, J. and Noilhan, J. (2000). From near-surface to root-zone soil moisture using year-round data, *Journal of Hydrometeorology*, 1(5), 393–411.

Ceballos, A., K. Scipal, W. Wagner, and J. Martıñez-Ferñandez (2005), Validation of ERS scatterometer-derived soil moisture data in the central part of the Duero Basin, Spain, *Hydrological Processes*, 19, 1549 – 1566.

Dawdy, D., and N. Matalas (1964), *Handbook of Applied Hydrology, A Compendium of Water-Resources Technology*, book chapter. Statistical and probability analysis of hydrologic data, part III: analysis of variance, covariance and time series., pp. 8.68–8.91, McGraw-Hill Book Company, New York.

Draper, C., Mahfouf, J.-F. and Walker, J. (2009). An EKF assimilation of AMSR-E soil moisture into the ISBA land surface scheme, *Journal of Geophysical Research*,114, D20104.

Habets, F., and co-authors (2008), The SAFRAN-ISBA-MODCOU hydrometeorological model applied over France, *Journal of Geophysical Research*,113, D06,113.

Kerr, Y., P. Waldteufel, J. Wigneron, J. Martinuzzi, J. Font, and M. Berger (2001), Soil moisture retrieval from space: The Soil Moisture and Ocean Salinity (SMOS) mission, *IEEE Transactions on Geoscience and Remote Sensing*, 39 (8), 1729–1735.

Mahfouf, J.-F., Bergaoui, K., Draper, C., Bouyssel, C., Taillefer, F. and Taseva, L. (2009). A comparison of two off-line soil analysis schemes for assimilation of screen-level observations, *Journal of Geophysical Research*, 114, D08105.

Masson, V., J.-L. Champeaux, F. Chauvin, C. Meriguet, and R. Lacaze (2003), A global database of land surface parameters at 1-km resolution in meteorological and climate models, *Journal of Climate*, 16 (9), 1261 – 1282.

Sabater, J., L. Jarlan, J.-C. Calvet, F. Bouyssel, and P. De Rosnay (2007). From near-surface to root-zone soil moisture using different assimilation techniques, *Journal of Hydrometeorology*, 8(2), 194–206.

Naeimi, V., K. Scipal, Z. Bartalis, S. Hasenauer, and W. Wagner (2009), An improved soil moisture retrieval algorithm for ERS and METOP Scatterometer observations, *IEEE Transactions on Geoscience and Remote Sensing*, 47, 1999–2013.

Noilhan, J., and J. Mahfouf (1996), The ISBA land surface parameterisation scheme, *Global and Planetary. Change*, 13, 145–159.

Noilhan, J., and S. Planton (1989), A simple parameterization of land surface processes for meteorological models, *Monthly Weather Review*, 117 (3), 536–549.

Pellarin, T., J.-C. Calvet, and W. Wagner (2006), Evaluation of ERS Scatterometer soil moisture products over a half-degree region in southwestern France, *Geophysical Research Letters*, L17401.

Quintana-Seguí P., P. Le Moigne, Y. Durand, E. Martin, F. Habets, M. Baillon, C. Canellas, L. Franchisteguy, and S. Morel (2008), Analysis of near-surface atmospheric variables: validation of the SAFRAN analysis over France, *Journal of Applied Meteorology and Climatology*, 47 (1), 92–107.

Reichle, R., and R. Koster (2004), Bias reduction in short records of satellite soil moisture, *Geophysical Research Letters.*, 31 (19), L19501.

Rüdiger, C., J.-C. Calvet, C. Gruhier, T. Holmes, R. de Jeu, and W. Wagner (2009), An intercomparison of ERS-Scat and AMSR-E soil moisture observations with model simulations over France, *Journal of Hydrometeorology*, 10 (2), 431–447.

Scipal, K., T. Holmes, R. de Jeu, V. Naeimi, and W. Wagner. A possible solution for the problem of estimating the error structure of global soil moisture data sets, *Geophysical Research Letters*¸ 35, L24403.

Seuffert, G., Wilker, G., Viterbo, P., Drusch, M. and Mahfouf, J.-F. (2004). The usage of screen-level parameters and microwave brightness temperature for soil moisture analysis, *Journal of Hydrometeorology*, 5(3), 516—531.

Sinclair, S., and Pegram, G. (2010), A comparison of ASCAT and modelled soil moisture over South Africa, using TOPKAPI in land surface mode, *Hydrology and Earth System Sciences*, 4, 613-626.

Vinnikov, K., and I. Yeserkepova (1991), Soil moisture: Empirical data and model results, *Journal of Climate*, 4, 66–79.

Wagner, W., G. Lemoine, and H. Rott (1999), A method for estimating soil moisture from ERS Scatterometer and soil data, *Remote Sensing of Environment*, 70 (2), 191–207.

Wagner, W., V. Naeimi, K. Scipal, R. de Jeu, and J. Martıñez-Ferñandez (2007), Soil moisture from operational meteorological satellites, *Hydrogeology Journal*, 15 (1), 121–131.

Wagner, W., Z. Bartalis, V. Naeimi, S.-E. Park, J. Figa-Saldaña, and H. Bonekamp (2010), Status of the MetOp ASCAT soil moisture product, *2010 IEEE International Geoscience and Remote Sensing Symposium, Hawaii*, 25-30 July 2010, Abstract number 3916.

Walker, J. and Houser, P. (2004), Requirements of a Global Near-Surface Soil Moisture Satellite Mission: Accuracy, Repeat Time, and Spatial Resolution, *Advances in Water Resources*, 27, 785-801.